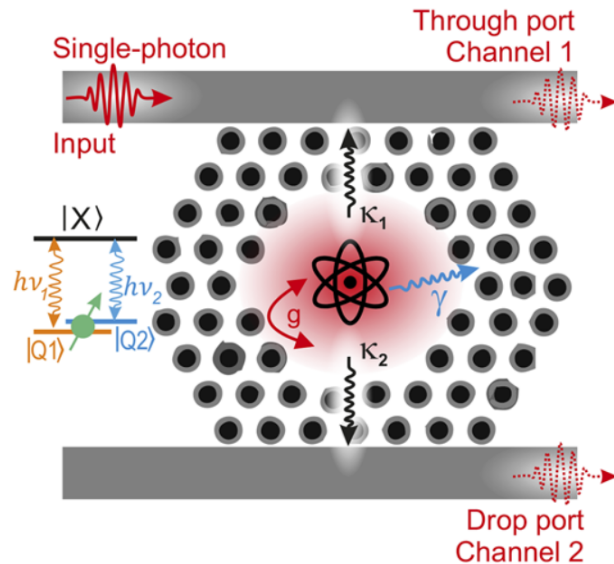


Photon Mediated Spin Qubits



Julie Belleville, Stephen Cashen, James Wu, Sarvan Gill

Project Sponsors:

Dr. Jeff Young - Project Lead Dr. Andreas Pfenning - Postdoc Researcher

ENPH 479 - Project 2154

April 10th, 2022



Executive Summary

Measurement based quantum computing is a new and promising technology that has many advantages over classical computing. Quantum computing leverages quantum mechanics principles such as superposition and entanglement and can, in principle, leverage an exponentially greater computational space than its classical counterpart. However, quantum computing technologies are today in their infancy and many competing architectures are being explored by researchers across the world.

Researchers at the Stewart Blusson Quantum Matter Institute (QMI) at UBC are working on implementing a measurement-based quantum computing architecture on a nanophotonic platform. Specifically QMI is looking into using emitters placed in silicon photonic crystal cavities as qubits, where qubit interactions (measurements) will be mediated by photons. To design their quantum architecture, QMI needs to understand the intricacies of the qubit, where potential errors come from, and how to quantify these errors for the purposes of error correction.

Our team was tasked with modelling and analysing the two main qubit systems (each associated with a given measurement) as well as with designing error metrics to accurately quantify errors in the system, such that our sponsors can understand how certain system parameters impact errors. Through our analysis, we examined potential designs of the cavity quantum electrodynamic system, and applied physical intuition, symmetry analysis, and numerical simulations to analyze different systems. Furthermore, we implemented software for a general simulation and sweep framework on systems of interest, and performed parameter sweeps to calculate expected transmission probabilities and corresponding error metrics. We essentially created a software system that allows QMI to investigate the errors of systems with different parameters—our hope is that it will be used to perform further sweeps informed by the results in this report.

Table of Contents

Executive Summary	1
Table of Contents	2
Table of Figures	4
Introduction	5
Discussion	10
Theory	10
Normalization of Units	10
Systems of Interest	10
Model 1: Single-Emitter Z System	12
Model 2: Dual-Emitter Z and ZZ Systems	26
Model 2B: Dual-Cavity, Dual-Emitter ZZ System	39
Conclusion	41
Recommendations	41
Future Work	42
Deliverables	42
Appendix A: Testing and Validation	43
Appendix B: Hamiltonian, Symmetry Analysis, and Theory for Models	45
Model 1	45
Model 2	46
Model 2B	47
Appendix C: Software Package	49
Appendix D: Background Theory	52
Input output Model	52
Scattering Matrices	52

S and M matrices	54
Error Metrics	54
References	59

Table of Figures

Title	Pg
Figure 1: Silicon Photonic Cavity	6
Figure 2: Z System	7
Figure 3: ZZ System	8
Figure 4: Z system and ZZ system with ports labelled	11
Figure 5: Model 1 setup	12
Figure 6: Transmission patterns with a fully on-resonance emitter	15
Figure 7: Transmission patterns with a fully off-resonance emitter	16
Figure 8: Effects of emitter detuning at different cooperativities	18
Figure 9: Transmission at various frequency detuning	19
Figure 10: Model 1 transmission probabilities with the photon input at port 1 (on-resonance)	21
Figure 11: Model 1 transmission probabilities with the photon input at port 2 (on-resonance)	22
Figure 12: Model 1 transmission probabilities with the photon input at port 1 (off-resonance)	23
Figure 13: Error metric sweeps for the one-emitter two-mode Z system	25
Figure 14: Model 2 Setup	26
Figure 15: Model 2 transmission for each port	28
Figure 16: ZZ system transmission with all emitters on-resonance	29
Figure 17: Error metric sweeps for the two-emitter two-mode Z system	30
Figure 18: Model 2 transmission probabilities with the photon input at port 1	31
Figure 19: Model 2 ZZ transmission probabilities with the photon input at port 1	33
Figure 20: Monte Carlo simulation of Z system transmission	37
Figure 21: Monte Carlo simulation of ZZ system transmission	37
Figure 22: Error metric sweeps for the ZZ system, with symmetrically-parametrized Z halves	38
Figure 23: Alternate 2-cavity 2-emitter 2-mode single Z system setup	40

Introduction

Background

Quantum computing is a fairly new technology and is particularly interesting as different groups are taking different approaches to their implementation. In classical computing, the fundamental building block is the classical bit. Even though a classical bit can only hold binary information, using many of these bits together can allow for complex computations. In quantum computing, the fundamental building block is the qubit. The qubit employs quantum properties such as superposition and entanglement so that its information space is exponentially larger than that of the classical bit. This has large implications as this building block has a larger capacity, which implies that quantum computers can do exponentially more complex computations and be more efficient than classical computers.

At the Stewart Blusson Quantum Matter Institute (QMI), Dr. Jeff Young and Dr. Andreas Pfenning are currently working towards creating a photonic measurement based quantum computing architecture.

Two common approaches to quantum computing architectures are circuit based and measurement based quantum computing. The circuit based model has been implemented in practice by a few companies and is more standard compared to the measurement based model. The architecture relevant to our report is measurement based quantum computing, in which entanglement and computation is applied through measurements.

Now, even within measurement-based quantum computing, there are many different potential architectures. QMI is looking specifically at photonic measurement-based quantum computers. Photonics is an area of study in physics that deals with the manipulation and creation of light and photons. These specific photonic measurement-based quantum computers use light and silicon based photonic cavities to entangle qubits and perform quantum measurements.

System of Interest

The physical representation of the qubit is shown in Figure 1.

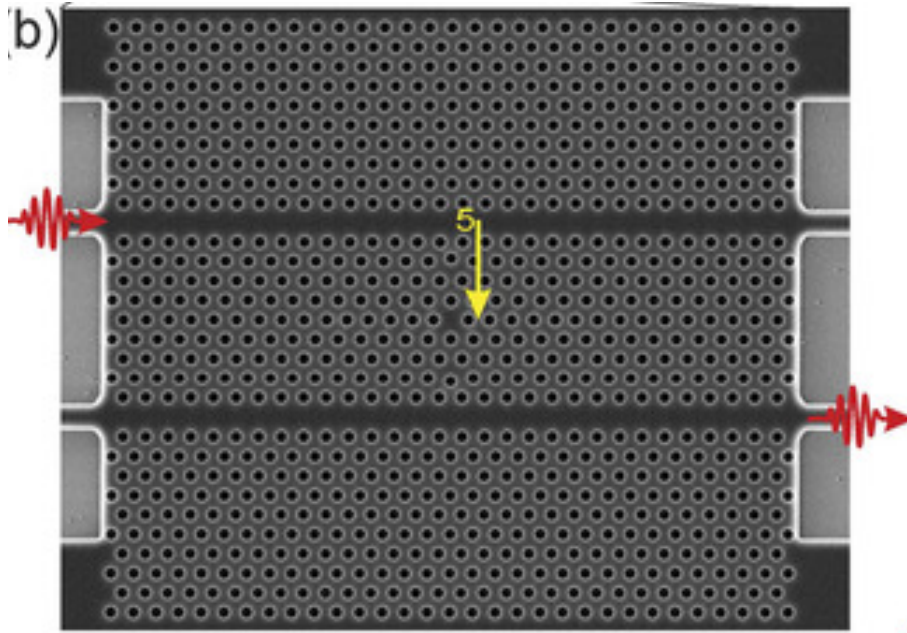


Figure 1: Diagram of a silicon photonic crystal cavity. The cavity is highlighted by the yellow arrow pointing to the break in the structure. Photons are shown by the red squiggly lines.

Figure 1 shows the structure of the silicon photonic crystal cavity, which will contain the qubit. In the figure, we can see that a break in the structure of the crystal creates a physical cavity. This cavity is surrounded by two waveguides, which photons can travel through. In this system, the state of the qubit is indirectly queried by sending a photon towards the cavity—if the qubit is in a state where it is on-resonance with the cavity, we want to design a system such that the photon remains in the waveguide in which it started; conversely, if the qubit is off-resonance with the cavity, we want the photon to switch to the opposite waveguide. This system with a single cavity is referred to as the Z system and is further explained below.

Z System

A simplified representation of the Z system is shown in Figure 2. The cavity is shown as a grey box with a purple atom (the qubit) inside. The photon's path is shown via the orange arrow. We refer to the top waveguide as the bus waveguide and the bottom waveguide as the drop waveguide, as labelled in Figure 3.

In this system, a photon enters through the bus waveguide travelling in the forward direction. In an ideal system, if the photons and the cavity are exactly on-resonance, the photon should be detected at the end of the bus waveguide. This is shown in Figure 2.1. In the opposite situation, if the photon and the cavity are off-resonance (i.e. their frequencies are sufficiently far), then the photon should drop through the cavity and go into the drop waveguide where we would detect it.

Now, if the photon's frequency is not precisely on- or off-resonance, the probability that it follows the ideal path is associated with the frequency difference.

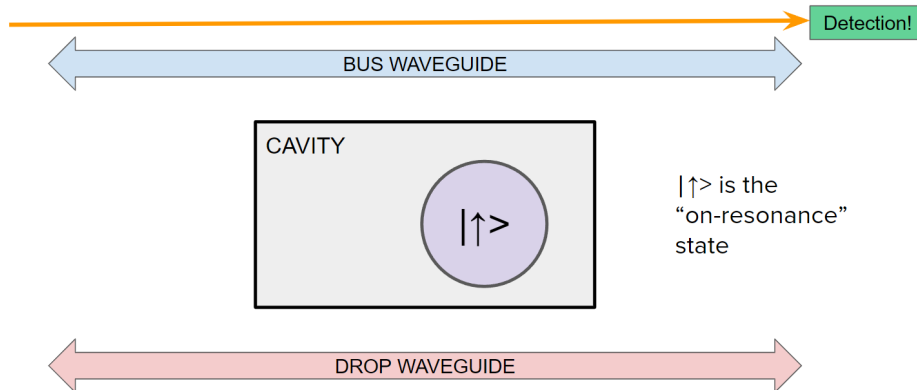


Figure 2.1: Z System (on-resonance state)

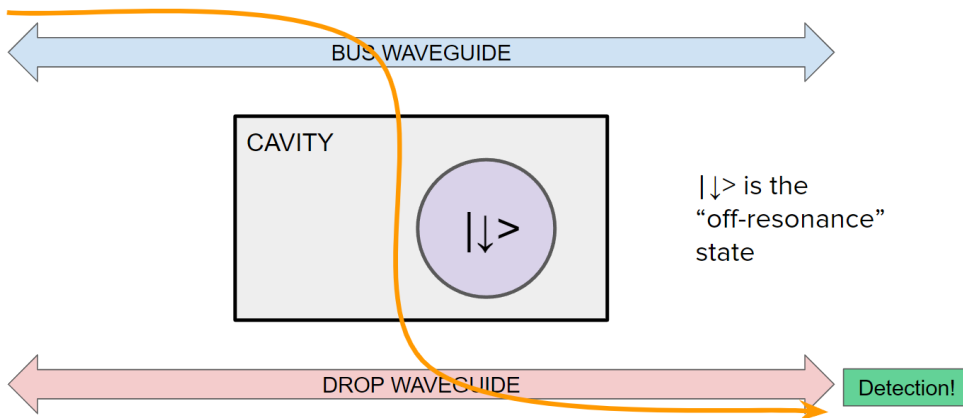


Figure 2.2: Z System (off-resonance state)

ZZ System

All quantum computing architectures must have a way of entangling qubits. This is done by using 2 cavities (i.e., putting two qubits side by side) and making our measurement at the end of the second qubit. This system is called the ZZ system and is shown in Figure 3 (there are two ZZ systems shown, one on top and one on the bottom). This figure shows how we can entangle two qubits in the ZZ system. If we look at the system at the top, we can see that if we measure a photon at the end of the bus waveguide, this means that the photon has either interacted with both cavities and remained in the bus waveguide or has dropped through both cavities and ended switched waveguides twice. So by measuring the photon in the bus

waveguide, we know that both of the qubits are in the same state. On the contrary, the bottom system shows that if a photon is measured at the end of the drop waveguide, the qubits have opposite states.

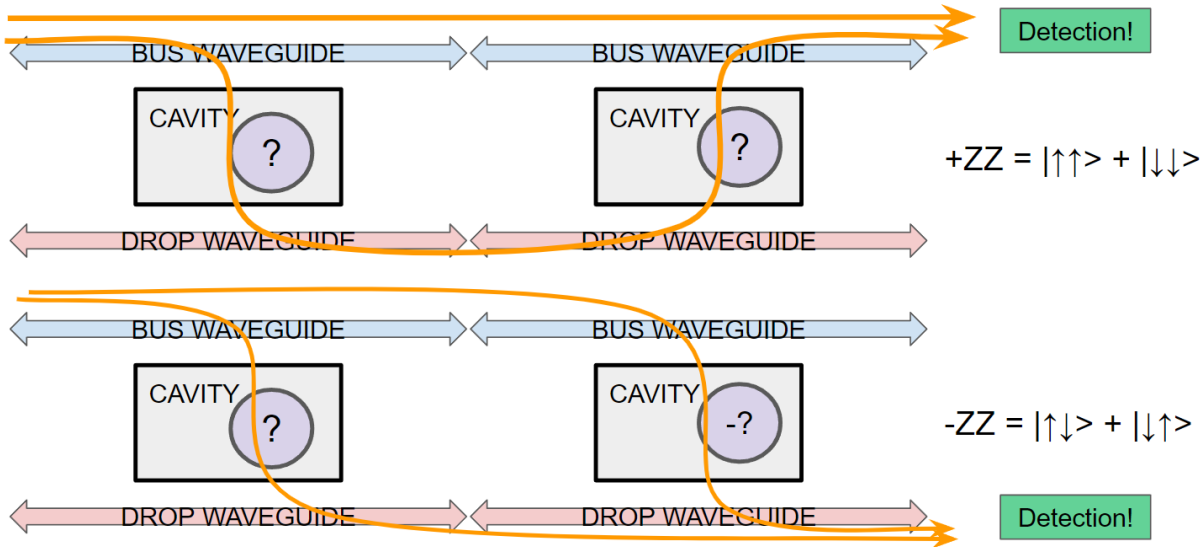


Figure 3: ZZ System and Entanglement

Project Goals

To create a quantum computing architecture with this system, QMI needs to be able to understand and model the interactions between the photons and the cavities. To manufacture these qubits, QMI needs to understand where errors in this system come from and how to quantify these errors. Furthermore, they need to know what parameters of this system will impact the errors and how this occurs.

The descriptions in the **Z system** and **ZZ system** sections represent ideal behaviours. In practice, the probability of the photon exiting through the wrong port is non-zero—this error must be quantified as a function of system parameters (e.g. coupling and loss). Thus our goals for this project and this document are to:

1. Model the behaviour of the Z and ZZ systems
2. Investigate engineering concerns (software parameter sweep)
3. Investigate error metrics to quantify the performance of these systems

Scope and Limitations

The scattering matrix framework is highly flexible, and we have only analyzed our system as a special case of the full framework. In particular, we limit ourselves to considering only single-photon interactions.

Multi-photon interactions are important higher-order terms in a full description of the system. We further assume that our input state is a single frequency, infinite time-continuous wave. A realistic finite-bandwidth pulse would behave less ideally than what our model predicts. We assume no time dependence in our system, such as thermalization of the qubit.

We have not aimed to sweep over all interesting parameters, only illustrative examples. Code has been provided such that users can sweep over interesting parameters and new models as they need.

Useful figures of merit will depend on the error-correcting code used. We have discussed and recommended general error metrics but not application-specific ones.

The sweeps we have conducted are over parameter ranges that have not been physically correlated; they should only be considered as qualitative guidance on the sensitivities of the models and as examples of how to conduct future sweeps.

Discussion

Theory

The dynamic cavity QED systems can be modelled as a scattering problem where we calculate the transition amplitudes between an input state interacting with the system and an output state outgoing from the system. For our purpose, we will label the states interacting with the scattering cavity as “Ports.” Figure 4 illustrates the ports on both Z and ZZ systems. It is important to note that the states are characterized by the waveguide the photon is occupying and the direction it is travelling in, rather than by the position it enters or exits the system.

The probability amplitudes are encoded in a scattering matrix S whose elements S_{ij} are the probability amplitudes that a photon will transition from port (state) i to port (state) j .

The theory of scattering matrices is well developed. An extremely general description of the formalism is derived in (Trividi, 2018), but a more accessible description can be found in (Gitt, 2021). We describe the formalism in broad strokes in Appendix D.

In the same appendix, we also include a discussion of error metrics, which can be used to convert the scattering matrix result into performance metrics for the whole system.

Normalization of Units

When viewing the presented results, it is important to note two things. The absolute frequency of the system is not relevant to its dynamics—only differences in frequency are. Therefore all frequencies are presented as detunings from a fixed frequency Ω_R . Furthermore, the system is also invariant to the choice of units, and only the ratios between values are relevant in the dynamics. Therefore all results will be presented as a ratio of a reference frequency κ_R .

When relevant, it should be assumed that we are working in $c=\hbar=1$ units.

Systems of Interest

Using the theory above, we proceed to analyze two systems of interest. As previously mentioned, we are interested in a 4-port system in which the probability of the photon exiting through each port is governed by the state of an emitter (Figure 4), which acts as a qubit in our quantum computation.

In an ideal version of our Z system (single-qubit system), where the input photon comes in port 1, we expect to see the output photon in port 1 (if the emitter is on-resonance with the rest of the system) or in port 3 (if the emitter is off-resonance with the rest of the system) with unity probability.

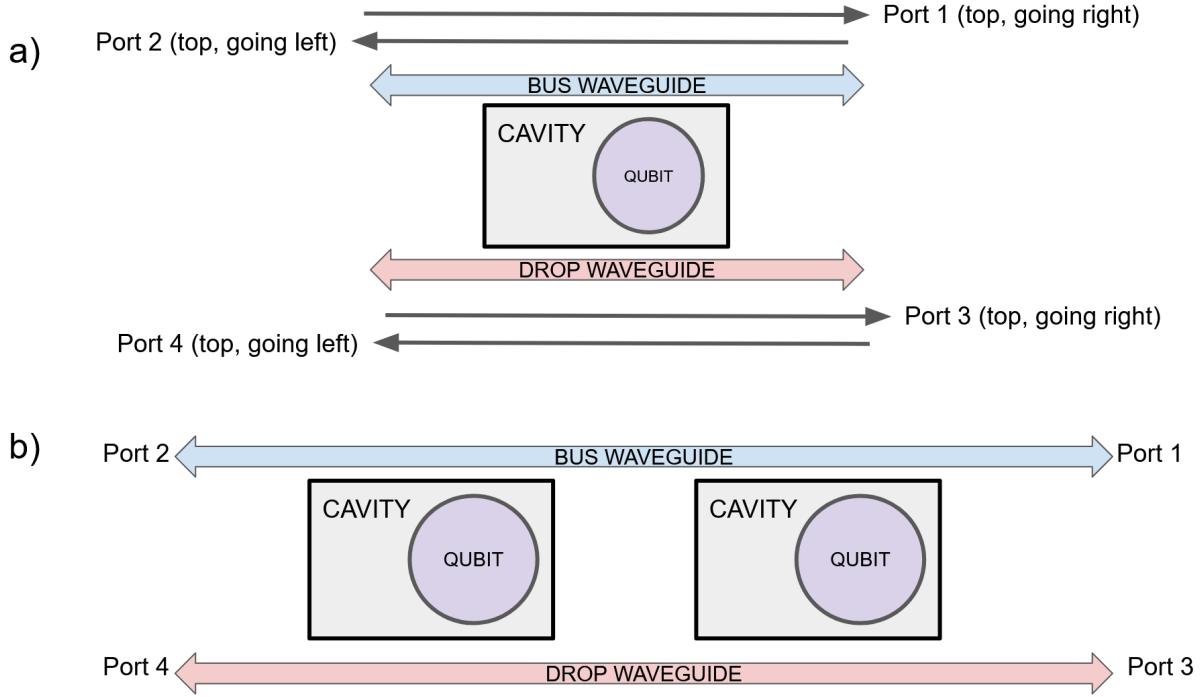


Figure 4: Z system (a) and ZZ system (b) with ports labelled. The ports are labelled both by position (bus or drop waveguide) and by direction of propagation.

In an ideal version of our ZZ system (2-qubit system) where the input photon comes in port 1, we expect to see the output photon in port 1 (if the 2 qubits are in the same state) or port 3 (if the 2 qubits are in opposing state) with unity probability.

We study 3 systems of interest below. In the following analysis, we consider both the systems' capability to provide the desired switching behaviour and their tolerance to error (e.g. frequency detuning or varying coupling strengths). The three systems we have chosen to study as candidates for further investigation are:

1. Model 1 (Z system candidate): single-qubit system with 4 ports, 2 modes, and 1 emitter
2. Model 2 (Z system candidate): single-qubit system with 4 ports, 2 modes, and 2 emitters (note that the two emitters would form a single logical qubit).
3. Model 3 (ZZ system candidate): two-qubit system with 4 ports, 2 modes, 2 emitters in each qubit system (i.e. two concatenated Z systems).

Of course, there are other setups that may also be good candidate implementations of our desired Z and ZZ systems. This report will therefore present a general software framework capable of simulating the single-excitation behaviour of a system with an arbitrary number of ports, cavity modes, and emitters; this software will also be able to calculate the behaviour of an arbitrary number of concatenated cavities.

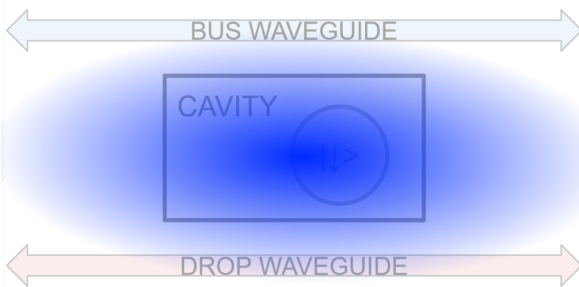
Note: as previously explained, all frequencies are expressed dimensionally as $\omega = \frac{\omega_{\text{true}} - \Omega_R}{\kappa_R}$.

Model 1: Single-Emitter Z System

System Overview

The first model we propose is a Z system candidate with 4 ports, 1 emitter, and 2 modes. We consider a cavity with an even mode and an odd mode (see Figure 5) following Fan et al.'s work on frequency-specific nanocavity-based drop ports (Fan 1998b). Interference effects coming from this symmetry will allow a photon input on-resonance with the cavity port modes into port 1 to exit only through port 3 (see Figure 4 for the port labels).

a) Even mode



b) Odd mode

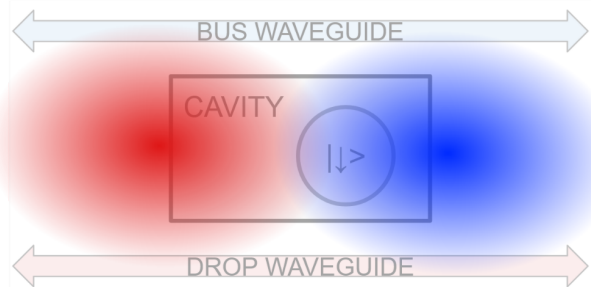


*Figure 5: Model 1 setup. The cavity couples to 2 waveguides (4 ports) and contains a single emitter. The cavity is designed with two same-frequency modes—one even (a) and one odd (b). Note that this figure is purely for illustrative purposes and that the shape and intensity of modes **does not** accurately reflect modes we expect to see in a cavity. The position of the emitter also does not necessarily reflect its physical positioning in the system.*

The system behaviour will then switch as follows with the emitter state. Suppose that a photon is input through port 1 at frequency Ω_R , and that Ω_R is also the frequency of the cavity modes when the cavity is empty. Then:

1. When the emitter is detuned from the cavity modes, it has minimal effects on the cavity modes, which remain at Ω_R . Then, the photon couples into the cavity, and is output at port 3 due to interference effects.
2. When the emitter is on-resonance with the cavity modes, it splits the cavity mode frequencies and detunes them from their nominal value of Ω_R . Then, the photon does not couple into the cavity and exits through port 1.

Simulation Results

All simulations run here can be found under:

`/examples/report_sweeps/model1_ZsystemCandidate_4ports_2modes_1emitter.ipynb`

in the project repository.

Ideal Result

First, we consider a nominally “ideal” simulation, with no losses, high coupling between cavity modes and the emitter, and no unwanted detuning (but with “full” detuning of the emitter in the off-resonance case). We use the parameters outlined in Table 1. Subsequently, we see the results in Figures 6 and 7.

We notice that in this “ideal” case and at zero photon detuning, we get the desired behaviour by sending a photon in through either port 1 and 3: no transmission through the right-to-left ports and full switching between port 1 (photon stays in top waveguide) and port 3 (photon travels through bottom waveguide) when the emitter shifts from on-resonance to off-resonance.

We notice also that the emitter state does not in fact affect the predicted transmission at all when the photon is input through ports 2 and 4; that is, the system behaviour is asymmetric. In fact, it is impossible to construct a symmetric single-emitter system in which the emitter couples equally to both the odd and even cavity modes: in a symmetric system, the emitter must be placed at the centre of the cavity where the odd mode has no field—it thus follows that the system we defined cannot be symmetric. Critically, a symmetrically placed emitter cannot cause detuning in the odd mode at all, and thus cannot provide the switching behaviour we require from our Z system.

Is this lack of symmetry a problem? Strictly speaking, the quantum computing architecture for which we are performing this analysis only requires photons to propagate one way. However, whether this would lead to additional errors in cases of non-idealities such as back-reflection, and how to control which way the system exhibits the switching behaviour remains to be investigated.

Parameter	Set in software with:	Value	Description
ω_{emit}	dw_emit_ref	0 (on-resonance) 2000 (off-resonance)	Emitter detuning from the reference (normalized).
ω_{even}	dw_mode_ref	0	Even mode detuning from the reference
ω_{odd}	dw_mode_ref	0	Odd mode detuning from the reference (normalized)
g_{even}, g_{odd}	g_mode_emit	1	Coupling between both the even and odd cavity modes and the emitter
$\Gamma_{even}, \Gamma_{odd}$	mode_loss	0	Loss from the even and odd cavity modes
γ	emit_loss	0	Losses from the emitter
$\kappa_{f, even}$	waveguide_coupling_multiplier waveguide_coupling	$\frac{1}{\sqrt{2}} [1 1 1 1]$	Coupling of the fields (not the power) between the even mode and each waveguide. The elements of the vector are given as port 1, port 2, port 3, port 4
$\kappa_{f, odd}$	waveguide_coupling_multiplier waveguide_coupling	$\frac{1}{\sqrt{2}} [1 -1 1 -1]$	Coupling of the fields (not the power) between the odd mode and each waveguide

Table 1: Ideal parameters for Model 1 simulation

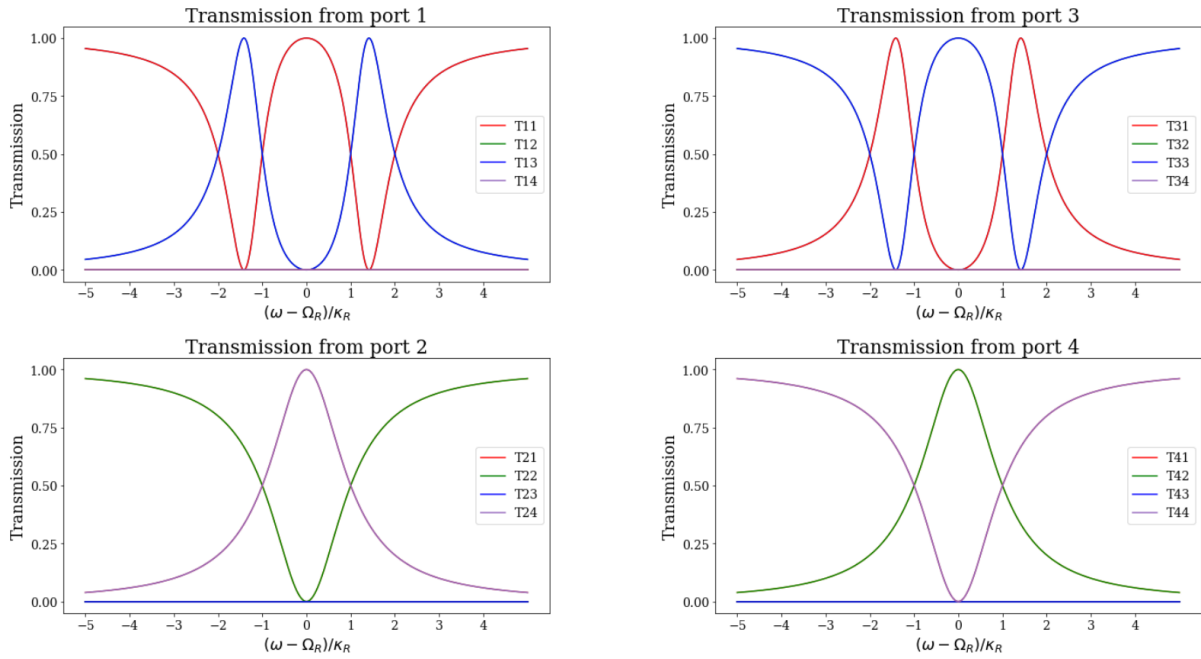


Figure 6: Transmission patterns with a fully on-resonance emitter. Transmission is plotted as a function of the photon detuning from reference frequency Ω_R , normalised by reference coupling coefficient κ_R in an ideal system with no loss.

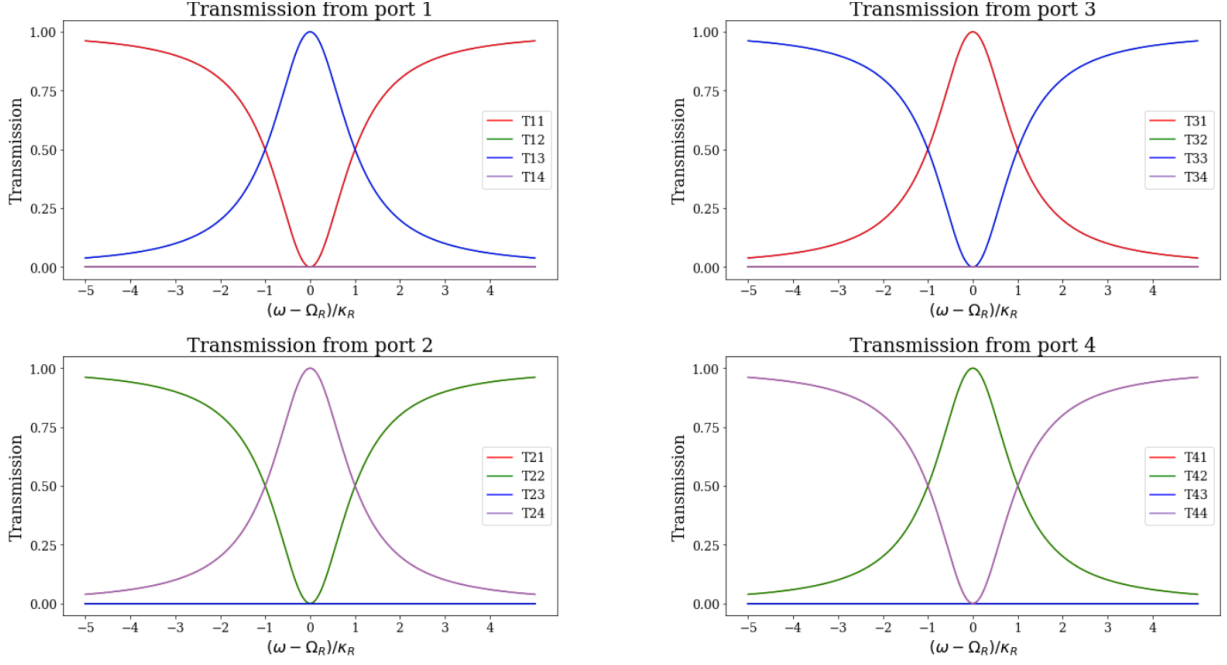


Figure 7: Transmission patterns with a fully off-resonance emitter. Transmission is plotted as a function of the photon detuning from reference frequency Ω_R , normalised by reference coupling coefficient κ_R , in an ideal system with no loss.

We note the following:

1. We can switch ports 1, 3 and 2, 4 (i.e. demonstrate the switching behaviour when the photon is input through 2 or 4 instead of 1 or 3) by setting either g_{even} or g_{odd} to a negative value (π phase between the two).
2. Similarly, we can switch ports 1, 3 and 2, 4 by changing $\kappa_{f, odd}$ from $\kappa_{f, odd} = \frac{1}{\sqrt{2}}[1 -1 1 -1]$ to $\kappa_{f, odd} = \frac{1}{\sqrt{2}}[-1 1 -1 1]$.

Cooperativity and Detuning

Next, we investigate the effects of emitter detuning on our system at different cooperativities. We will sweep over emitter detuning $\omega_{emit} \in [0.1, 0.5, 1.2, 2.4]$, with $C = \frac{g^2}{\kappa\gamma} \in [5, 100]$, with $\gamma = 1/100$. All other parameters remain the same as in Table 1 above (and can be viewed in our Jupyter Notebook).

From Figure 8 below, we note the following:

1. Increased detuning of the emitter shifts the transmission spectrum to be closer to the transmission spectrum of an empty cavity (for both cooperativity regimes).

2. The high-cooperativity case gives us a transmission spectrum which is significantly less sensitive to photon detuning. That is, a high-cooperativity system is more robust to any errors in input photon frequency.
3. The high-cooperativity behaviour changes much less than the lower-cooperativity behaviour for a given emitter detuning. Indeed, we see that a detuning of $\omega_{emit} = 1.2 \kappa_R$ at $C = 5$ fully switches the transmission probability of an input photon with no detuning, but that it puts the transmission probabilities at 50% port 1 and 50% port 3 at $C = 100$. Thus, a greater emitter detuning is required for the same switch in transmission probabilities at higher cooperativities.

This gives rise to an interesting engineering trade-off: a higher cooperativity means that the system will be more tolerant to errors in its photon source, but will also require a larger detuning between qubit states (and thus an emitter capable of supporting this detuning).

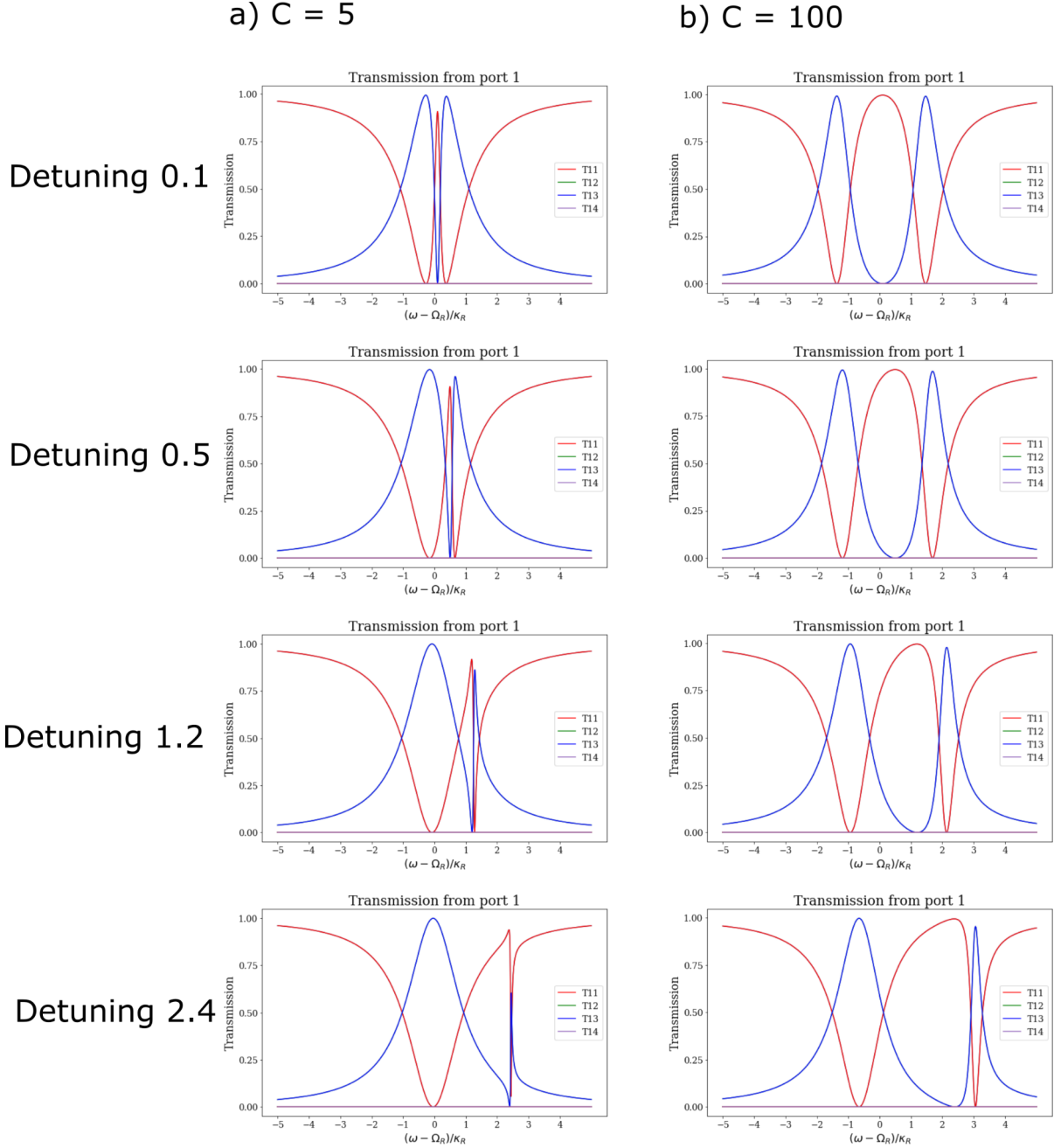


Figure 8: Effects of emitter detuning at different cooperativities. Transmission at all ports with port 1 as the input port, as a function of the photon detuning from reference frequency Ω_R normalised by reference coupling coefficient κ_R . On the left (a), we observe the effect of emitter detuning (normalised by κ_R) on the transmission probabilities at a cooperativity $C = 5$. On the right (b), we observe the same effects at $C = 100$. Only port 1 is shown (port 3 behaviour is the same as port 1, and ports 2 and 4's transmission probabilities do not shift with emitter detuning).

Mode Detuning

Next, we consider the difficulty of engineering cavity modes with specific frequencies. In the process of manufacturing such cavities, we can expect some frequency detuning between the actual cavity frequency and its engineered frequency. In Figure 9 below, we can see a plot where different lines correspond to different sets of odd and even mode detunings from the reference frequency:

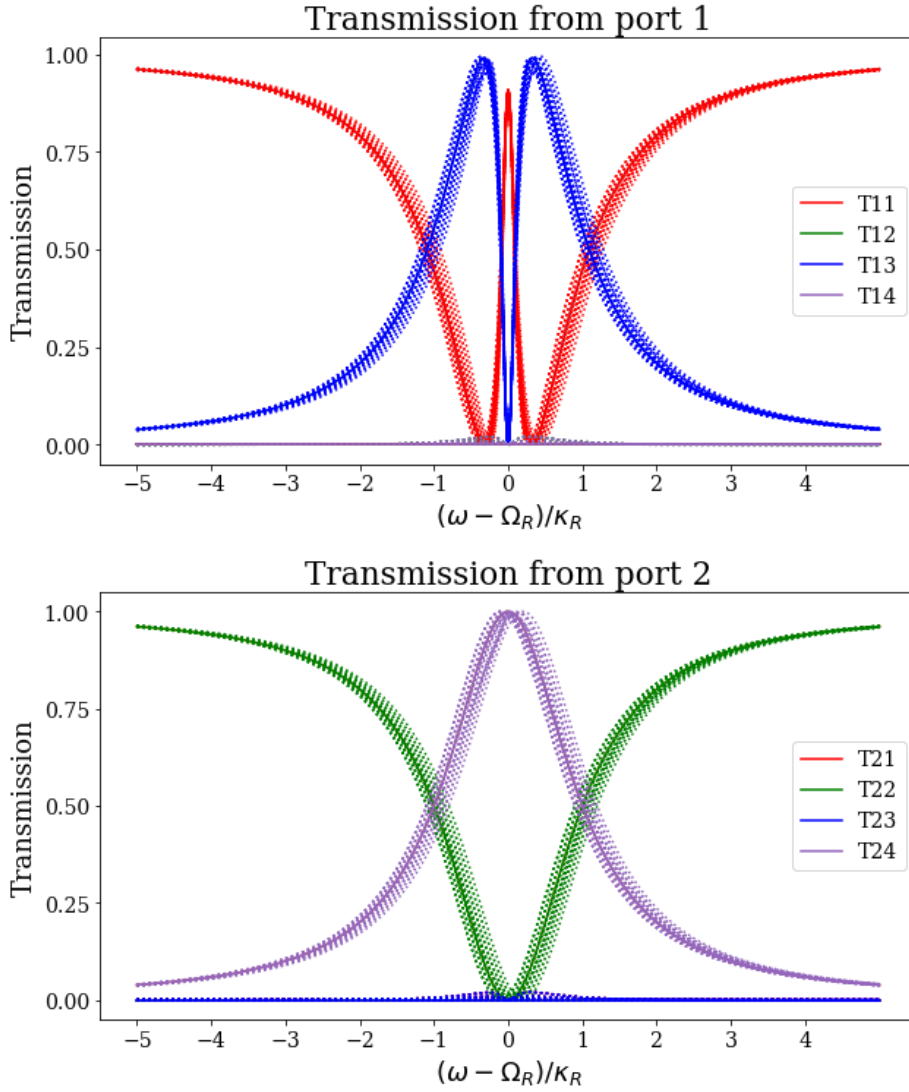


Figure 9: Transmission at various frequency detunings of the odd and even mode, where the detunings are every pair such that $\omega_{even}, \omega_{odd} \in [-0.2, -0.1, 0, 0.1, 0.2]$ (values given in our normalisation system). We see that mode detuning can shift our transmission peaks.

This sweep is run with an emitter loss of $\gamma = 1/100$, a mode-emitter coupling of $g_{even} = g_{odd} = \sqrt{5}/10$, cavity detuning frequencies as any pair where $\omega_{even}, \omega_{odd} \in [-0.2, -0.1, 0, 0.1, 0.2]$, and all other values as set in Table 1.

Emitter-Cavity Coupling Strength

We now consider how our system behaviour varies with changes in the strength of coupling between the even / odd modes and the emitter. Physically, the coupling of the emitter to different modes will strongly depend on its positioning in the cavity; since we expect variable emitter position as a result of the manufacturing process, we are interested in how this may affect our designed system.

From the Gitt thesis: the true parameter governing our system behaviour is the cooperativity

$$C = \frac{g^2}{\kappa^2 \gamma}$$

where g is the coupling between emitter and cavity mode and κ^2 is the total coupling of power. This becomes a bit more complicated with 2 modes (and indeed we have not gone through the analysis), but we will nonetheless restrict our sweep to modifying g only, under the assumption that it would be redundant to modify both g and κ^2 .

We set $\gamma = 1/100$ (normalised) in all plots for this section. Additionally, we set $\omega_{emit} = 2.4$ (normalised) in the detuned case, for a more realistic estimate of the switching behaviour.

In Figures 10-12, we observe the following:

1. As previously noted, the system behaviour is asymmetric (behaviour in the left-to-right ports differs from behaviour in the right-to-left ports)
2. The desired switching behaviour between the probabilities where the emitter is on-resonance and the probabilities where the emitter is off-resonance appears when the odd and even modes are equally coupled. When the coupling is significantly different, however, this switching behaviour fails to appear. This makes sense: when coupled unequally to the odd and even modes, the emitter shifts one of their frequencies more than the other, which reduces the destructive interference which allows us to control the direction of the photon output.
3. Also as previously noted, a higher coupling between emitter and cavity modes (i.e. a higher cooperativity) improves the transmission spectrum when the emitter is on-resonance, but makes it worse when the emitter is off-resonance, for a given detuning.

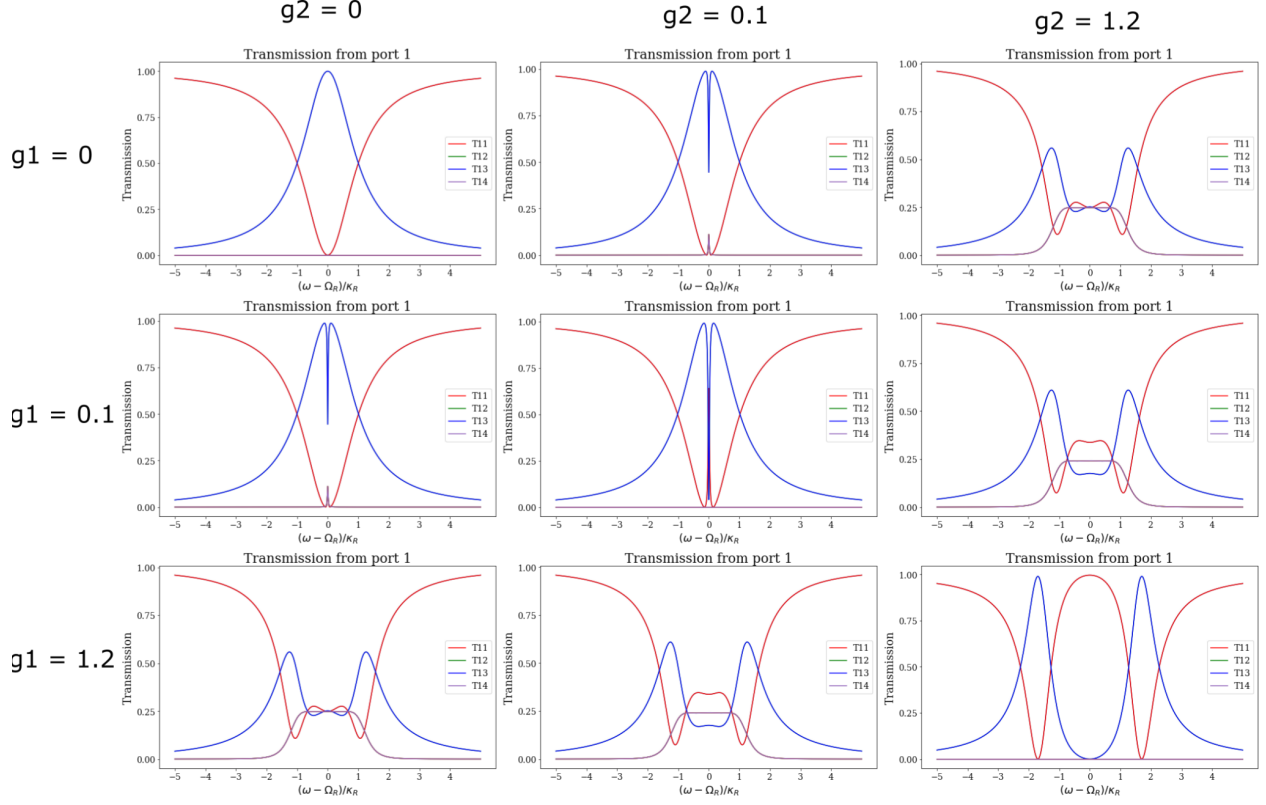


Figure 10: Model 1 transmission probabilities with the photon input at port 1 and the emitter on-resonance with the cavity frequencies, at various coupling strengths between odd and even modes of the cavity, and the cavity emitter. g_1 corresponds to the even mode, and g_2 to the odd mode. We note that the desired switching behaviour is achieved on the diagonal of the system, but that unequal coupling between the odd and even modes destroy the switching behaviour.

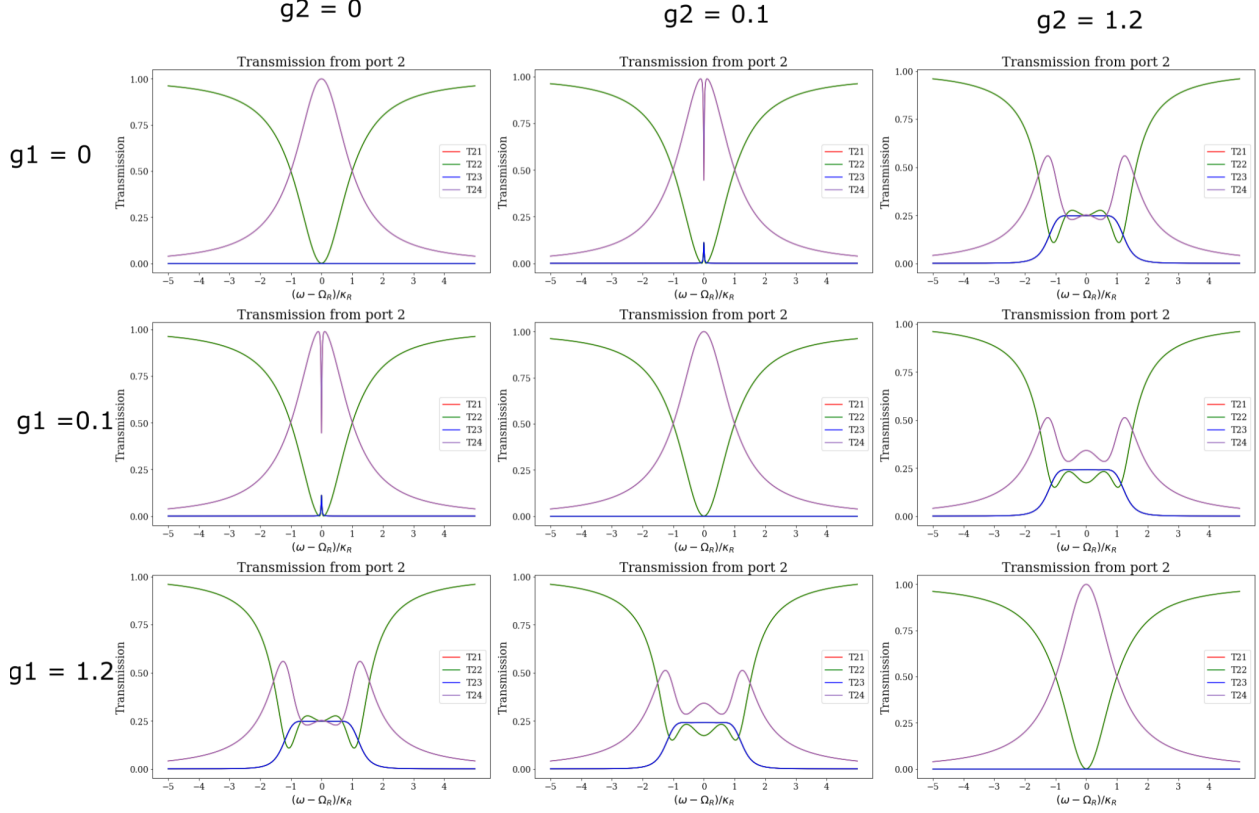


Figure 11: Model 1 transmission probabilities with the photon input at port 2 and the emitter on-resonance with the cavity frequencies, at various coupling strengths between odd and even modes of the cavity, and the cavity emitter. g_1 corresponds to the even mode, and g_2 to the odd mode. We note that the cavity behaves as if empty when $g_1 = g_2$

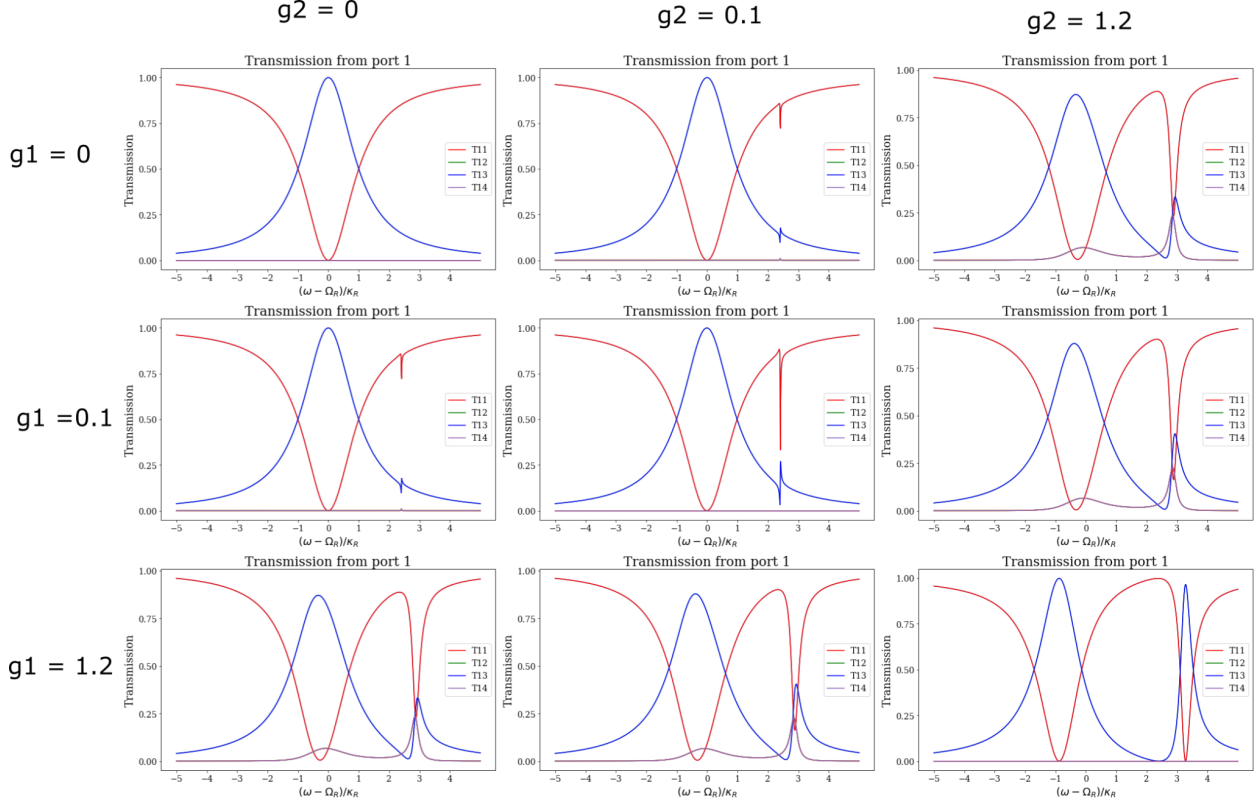


Figure 12: Model 1 transmission probabilities with the photon input at port 1 and the emitter off-resonance (detuning 2.4) with the cavity frequencies, at various coupling strengths between odd and even modes of the cavity, and the cavity emitter. g_1 corresponds to the even mode, and g_2 to the odd mode. We note that as the strength of coupling increases, the photon probabilities at Ω_R get further away from desired probabilities

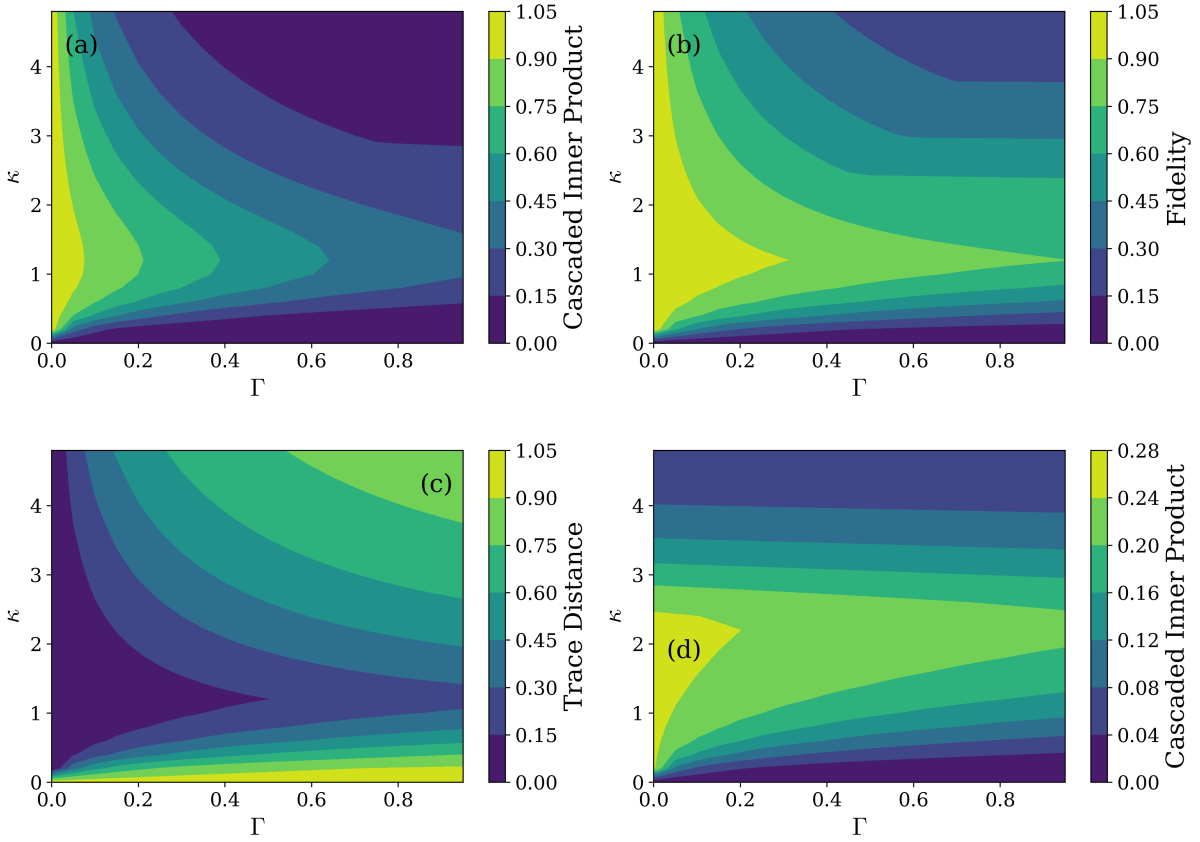
(which are $T_{13} = 1$, $T_{11} = 0$).

Note: we do not show the transmission probabilities where the photon is input at port 2 and the emitter is off-resonance, we those results look very similar to when the photon is input at port 1.

Error Metrics

The cascaded inner product, fidelity, and trace distance metrics are swept over waveguide-cavity coupling strength and system loss for the one-emitter Z system in Figure 13. The particular system parameters has $\kappa_{i,j} = \pm \kappa / \sqrt{2}$, where i, j index the waveguide and cavity modes while \pm is signed according to the parity of the coupled cavity mode. Meanwhile, the cavity modes and the emitter all exhibit a loss rate of Γ . From Figure 13, we see that in the presence of emitter-cavity coupling ($g = 1$), the three metrics generally agree with each other. Elsewhere, in the decoupled limit ($g = 0$), the cascaded inner product and fidelity agree as expected given how their difference lies only in the power scaling of the summed probabilities. However, the trace distance appears to be of lower resolution, as the effect of loss is lost (no pun intended) for the $g = 0$ case.

When there is emitter-cavity coupling, it appears that the waveguide-cavity coupling strength should be moderate (here $\kappa = 1$) for ideal performance—where there is little loss, the figures of merit are unity for the cascaded inner product and fidelity, and zero for the trace distance. In contrast, the ideal waveguide-cavity coupling becomes twice as strong in the absence of emitter-cavity coupling. The interpretation of this doubling is not particularly useful since the metrics are all quite poor (considerable deviation from unity/zero) when the emitter is decoupled from the cavity. This is unsurprising, considering that the emitter-cavity interaction is an important part of the system’s operation. Finally, smaller losses are seen to lead to better performance, which is consistent with how photon loss is a source of error. The ideal region of moderate waveguide-cavity coupling and low loss agrees with results from previous work (Gitt 2021).



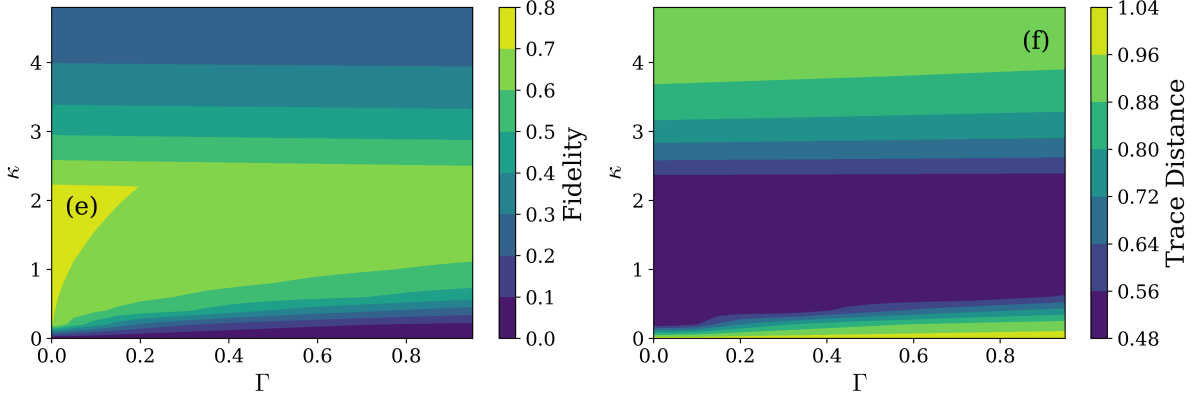


Figure 13: Error metric sweeps over cavity-waveguide coupling strengths and system loss for the one-emitter two-mode Z system. This is presented for various emitter-cavity mode coupling strengths: (a)-(c) $g = 1$, (d)-(f) $g = 0$. The units are normalised as discussed previously. Finally, the metrics are combined over all frequencies using a maximisation rule.

Single-Emitter Conclusions

This 1 emitter, 2 mode candidate for the Z system can in theory provide the required switching behaviour needed for the system, as long as we expect our architecture to be fully directional. However, it suffers from two potential disadvantages:

1. It is not clear, at this time, how easily engineered the directionality of the system is (it may be that small positional changes in how the system is manufactured will strongly impact the phase which determines the directionality). This system has a high sensitivity to phase of coupling.
2. Increased cooperativity means that the emitter detuning in the off-resonance case has to be increased as well, which imposes additional constraints on candidate emitters.
3. The cascaded inner product and fidelity agree in terms of identifying good-performing versus bad-performing systems. The trace distance has lower resolution compared to the other two, however. We therefore recommend the cascaded inner product and fidelity metrics; the subsequent sweeps are only performed with the cascaded inner product to avoid redundancy.
4. Moderate waveguide-cavity coupling and no loss is ideal for an emitter-cavity coupled Z system. Elsewhere, a Z system without emitter-cavity coupling is useless as one should expect.

Model 2: Dual-Emitter Z and ZZ Systems

System Overview

In Model 1, we discussed that the state of an emitter in a single-emitter symmetric system cannot switch the photon path as necessary for our quantum computing architecture. In this section, we propose a 2-emitter Z system with symmetric behaviour, capable of switching the photon path as needed.

To achieve this behaviour, we designed the system with 2 symmetrically placed emitters. Much like the modes, the emitters have an odd and even superposition. Then, we expect that the odd superposition of emitters will only couple with the odd cavity mode, and that the even superposition of the emitter will only couple with the even cavity mode. This system is shown in Figure 14:

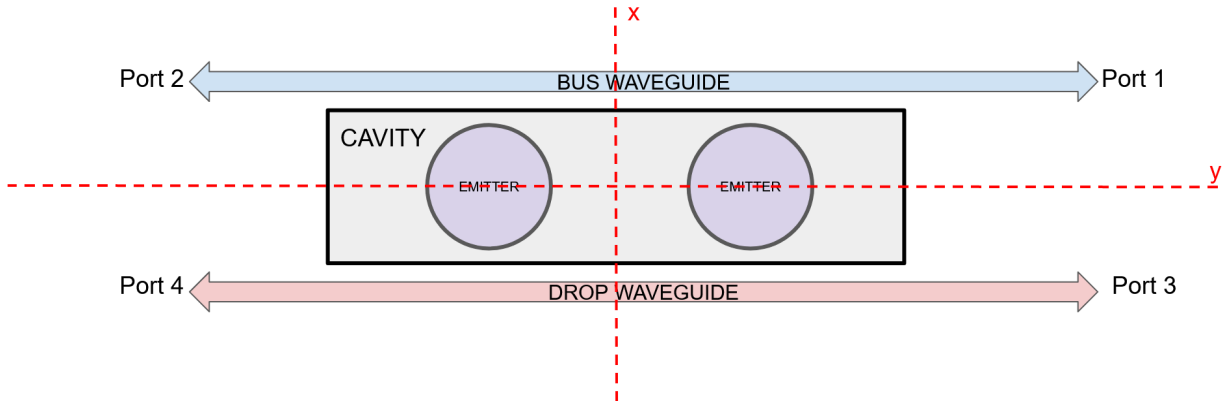


Figure 14.1: Model 2 Setup. The system contains 2 modes (one even and one odd) as well as 2 emitters which form an even and odd superposition. This proposed Z system allows us to restore the symmetry that Model 1 could not contain.

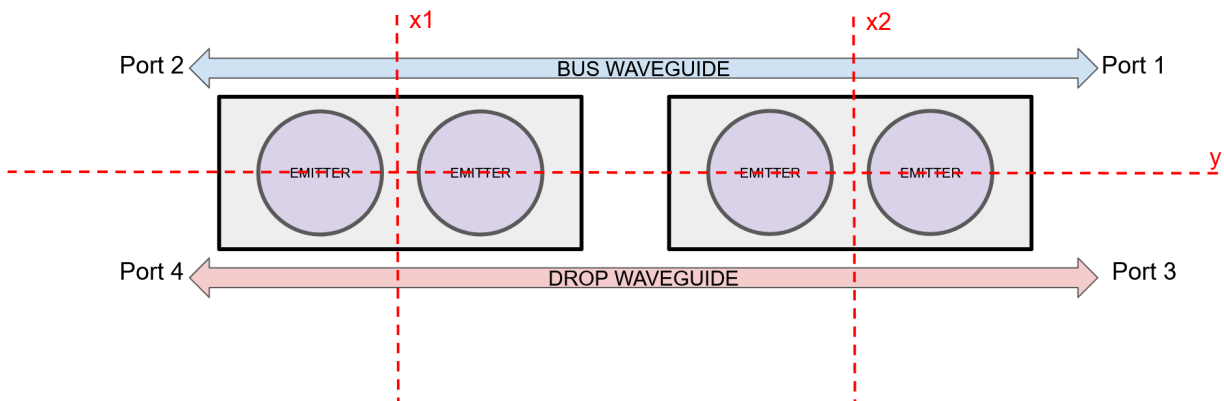


Figure 14.2: Model 2 ZZ system. The system contains 2 modes (one even and one odd) as well as 2 emitters which form an even and odd superposition in each cavity.

This time, we consider not only the Z system, but also its corresponding ZZ system (i.e. the system which results from the concatenation of two Model 2 Z systems). This serves 2 purposes:

1. Illustrates the behaviour we can expect from the ZZ system described, and allows us to make some observations.
2. Showcases our ability to use our SM matrix formalism to chain cavities

For a fuller theoretical discussion of this model see *Appendix B: Model 2*.

Simulation Results

All simulations run here can be found under:

`/examples/report_sweeps/model2_ZsystemCandidate_4ports_2modes_2emitters.ipynb`

in the software repository.

For this system, we focus our sweeps on the coupling between emitter and modes, and on a general Monte Carlo analysis of errors.

Ideal Result

As for Model 1, we consider the ideal case to start: no losses, high coupling between cavity modes and the emitter, and no unwanted detuning (with “full” detuning of the emitter in the off-resonance case). We use the same parameters as in Table 1, but with the following coupling coefficients:

$$g_{\text{emit1, mode even}} = 1$$

$$g_{\text{emit2, mode even}} = 1$$

$$g_{\text{emit1, mode odd}} = 1$$

$$g_{\text{emit1, mode odd}} = -1$$

We get the transmission spectrum shown in Figure 15, and see that indeed, adding a second emitter has allowed us to overcome the asymmetry imposed by Model 1. This is consistent with our symmetry analysis.

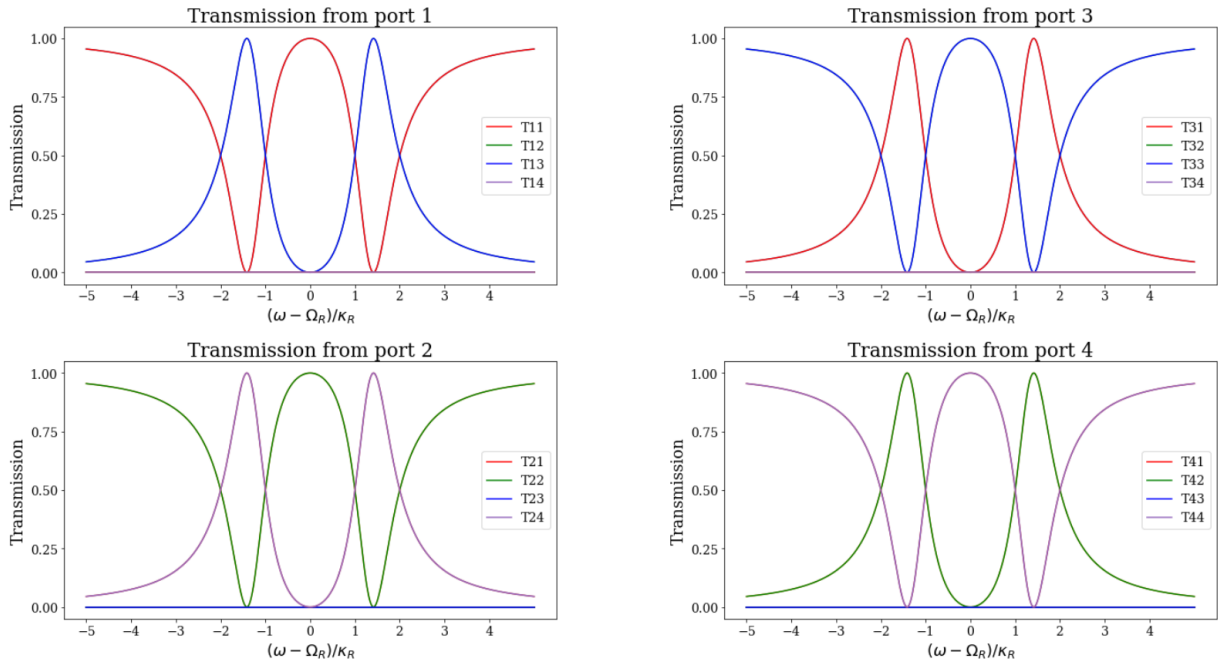


Figure 15.1: Model 2 transmission for each port, with the on-resonance emitter.

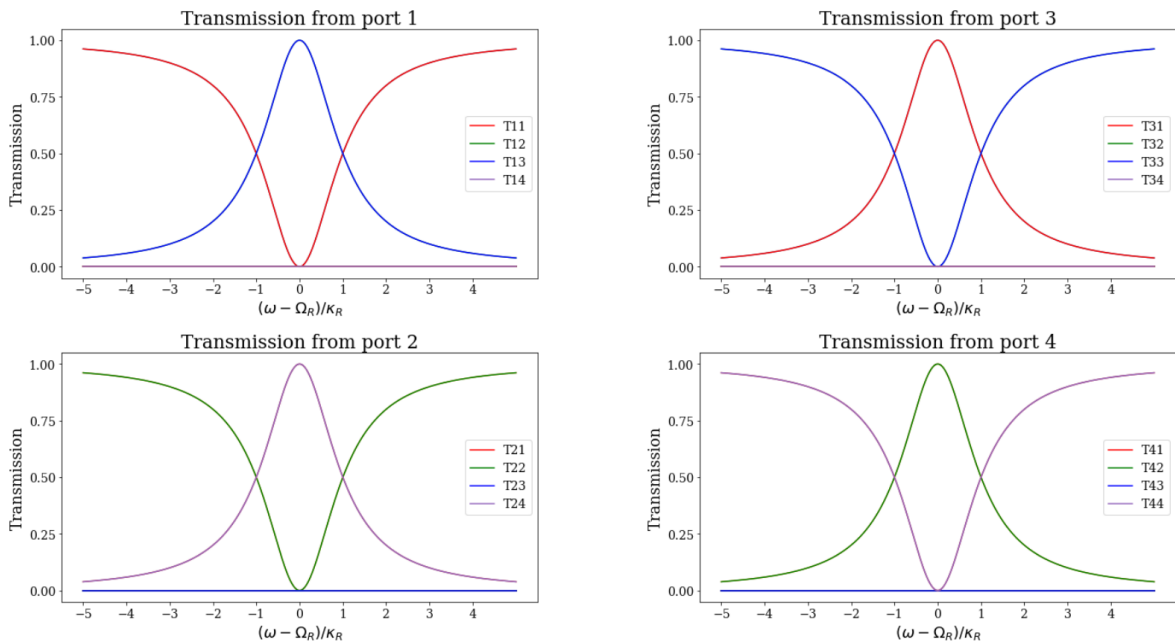


Figure 15.2: Model 2 transmission for each port, with the off-resonance emitter.

Using the S-matrix formalism outlined above, we consider the ZZ system produced by chaining 2 ideal Model 2 Z systems (see Figure 16). Since the behaviour is symmetric with respect to the ports, we only show the results where the photon is input through port 1:

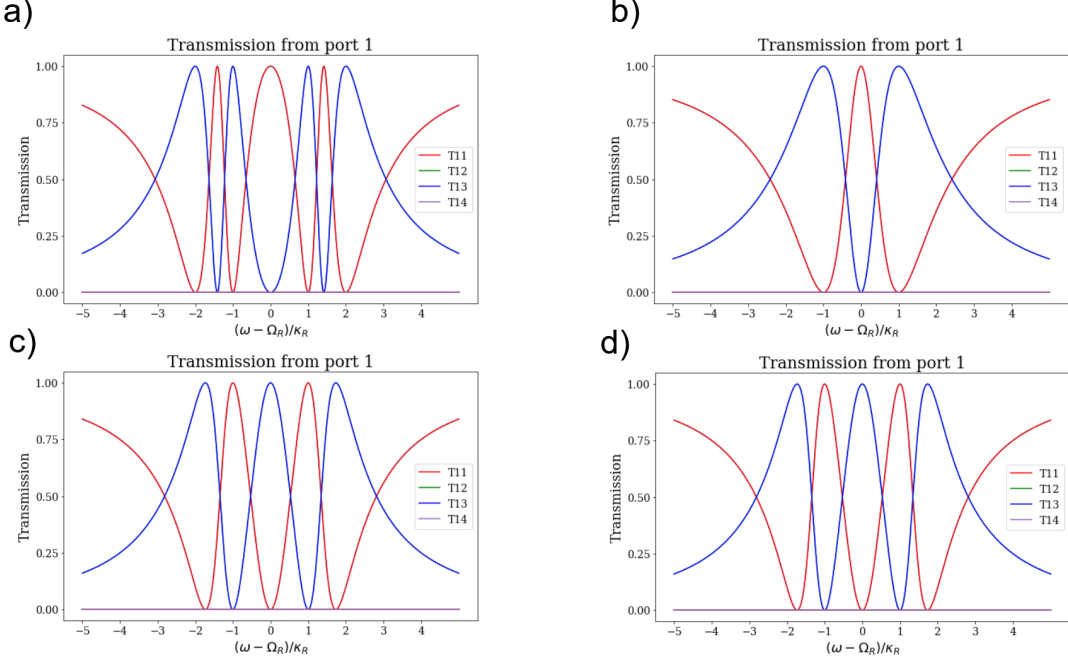


Figure 16: ZZ system transmission with all emitters on-resonance with the cavity (a), all emitters fully off-resonance with the cavity (b), the first and second Z systems on- and off-resonance, respectively (c), and the first and second Z systems off- and on-resonance, respectively (d).

As expected, we see in Figure 16 the photon remains in the top waveguide if both logical qubits (now each composed of 2 emitters) are in the same state, and drops to the bottom waveguide if the logical qubits are in opposite states.

We also note that the transmission peaks of the ZZ system are narrower than those of the Z system: this is important because this indicates that the ZZ system will tolerate significantly less detuning of the input photon than the Z system—we also expect that if systems are further concatenated (e.g. with three cavities in a row), this narrowing effect will become even more significant.

Z System Error Metrics

The cascaded inner product is again swept over waveguide-cavity coupling strength and system loss, this time for the two-emitter Z system in Figure 17. Again, the particular system parameters has $\kappa_{i,j} = \pm \kappa/\sqrt{2}$ and loss rate of Γ for both cavity modes and both emitters.

From Figure 17, we again see that emitter-cavity coupling ($g = 1$ for both emitters) is necessary for proper operation. When one or both emitters are decoupled from the cavity, the performance quickly deteriorates in the presence of just a bit of loss ($\Gamma \sim 0.02$). When $g = 1$ for both emitters, we again observe moderate cavity-waveguide coupling ($\kappa \sim 1$) and low loss to be optimal.

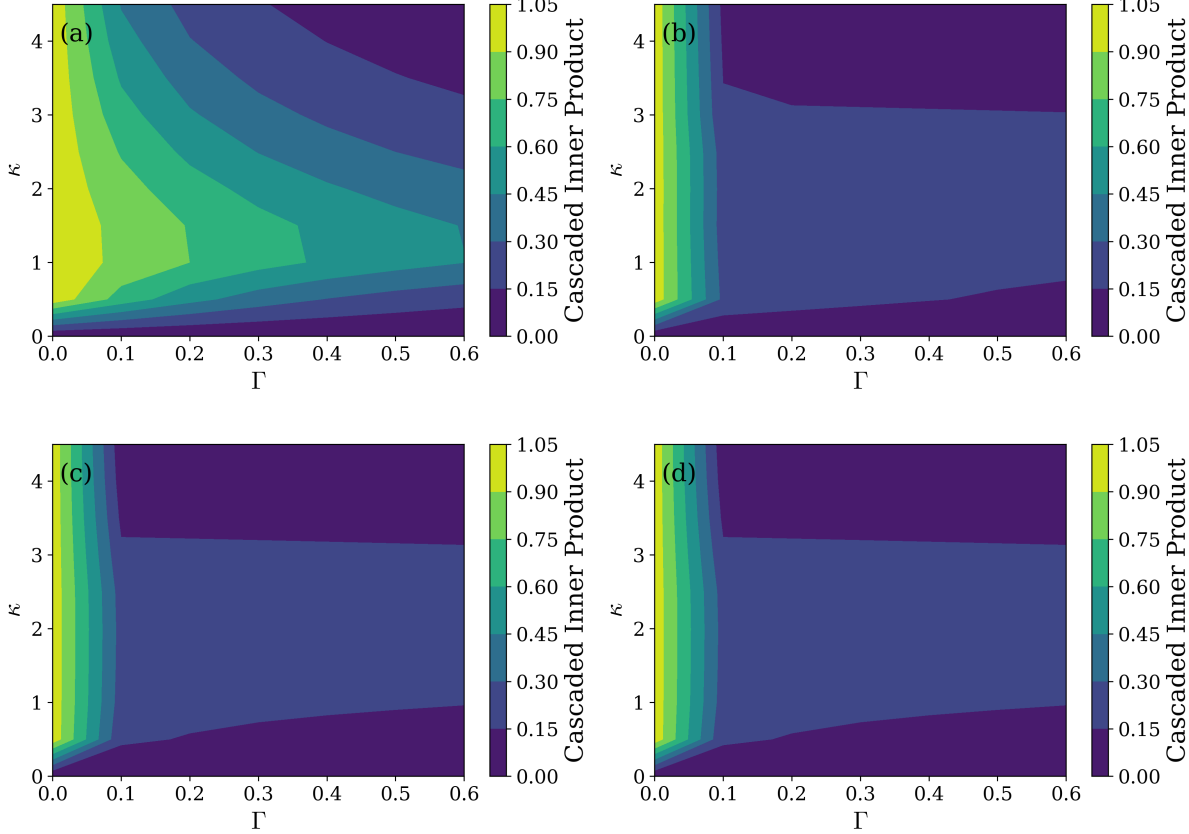


Figure 17: Error metric sweeps over cavity-waveguide coupling strengths and system loss for the two-emitter two-mode Z system. This is presented for various emitter-cavity mode coupling strengths: (a) $g_1 = g_2 = 1$, (b) $g_1 = 1, g_2 = 0$, (c) $g_1 = 0, g_2 = 1$, (d) $g_1 = g_2 = 0$. The units are normalized as discussed previously. Finally, the metrics are combined over all frequencies using a maximization rule.

Emitter-Cavity Coupling Strength

Next, we consider the behaviour of the system when the even mode to emitter coupling does not match the odd mode to emitter coupling, as we did for Model 1.

Again, we use the same parameters as in Table 1, but with both emitter losses set to $\gamma = 1/100$, and the following coupling coefficients:

$$g_{\text{emit1, mode even}} = g_1$$

$$g_{\text{emit2, mode even}} = g_1$$

$$g_{emit1, mode odd} = g_2$$

$$g_{emit1, mode odd} = -g_2$$

where g_1, g_2 is every pair of values such that $g_1, g_2 \in [0, 0.1, 1.2]$.

From Figure 18, we note the following:

1. Unlike in Model 1, even if the coupling coefficients are unequal, we see that at no photon detuning there seems to be a peak of T11 transmission that we want. Take for example $g_1 = 0.1, g_2 = 1.2$: even though the central peak does not seem to hit unity transmission, it nevertheless exists (unlike in the equivalent example of Model 1).
2. Also unlike Model 1, we see back reflections in the system when $g_1 = g_2$.
3. As observed in Model 1, higher cooperativity setups require more emitter detuning to return to “empty” cavity behaviour at no photon detuning.

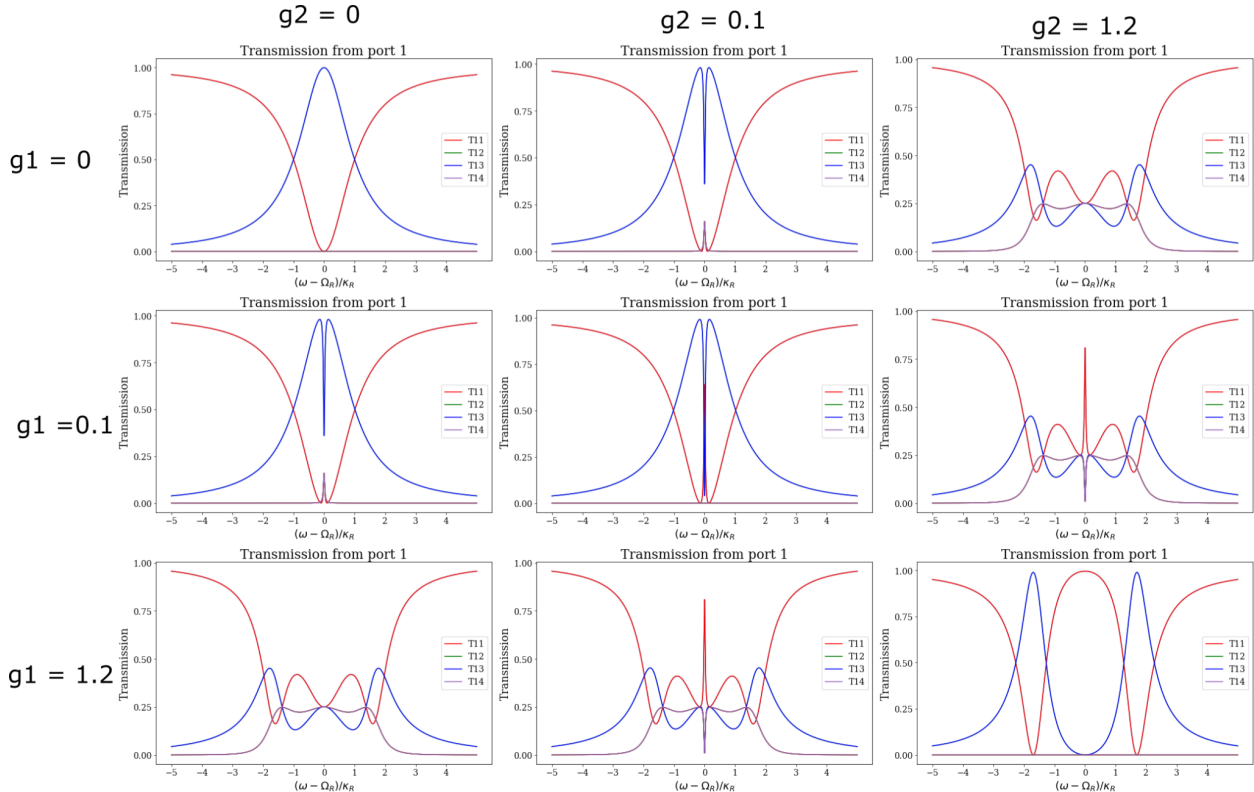


Figure 18.1: Model 2 transmission probabilities with the photon input at port 1 and the emitters on-resonance with the cavity frequencies, at various coupling strengths between odd and even modes of the cavity and the pair of emitters.

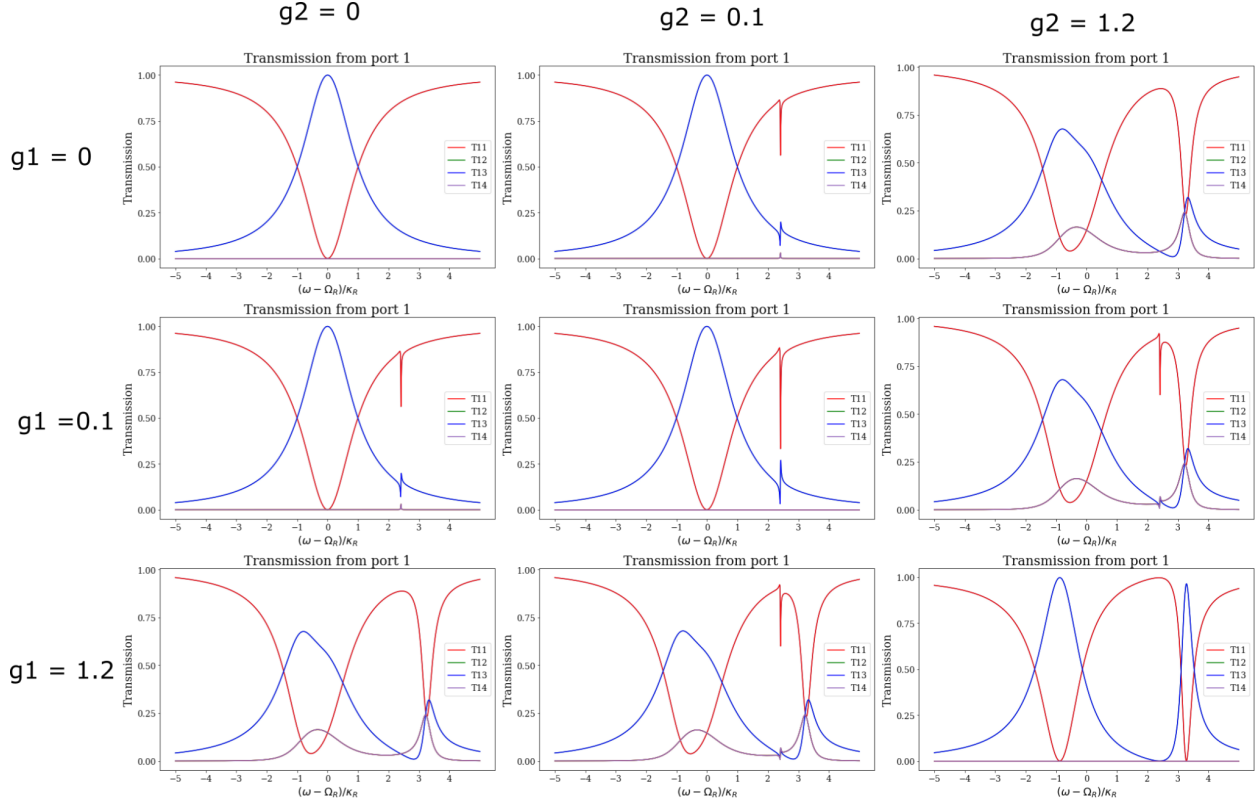


Figure 18.2: Model 2 transmission probabilities with the photon input at port 1 and the emitters off-resonance (detuning 2.4 for each emitter) with the cavity frequencies, at various coupling strengths between odd and even modes of the cavity and the pair of emitters.

We now look at the effects on the ZZ system in Figures 19 and observe that issues observed in the Z system transmission tend to be exacerbated in the ZZ system.

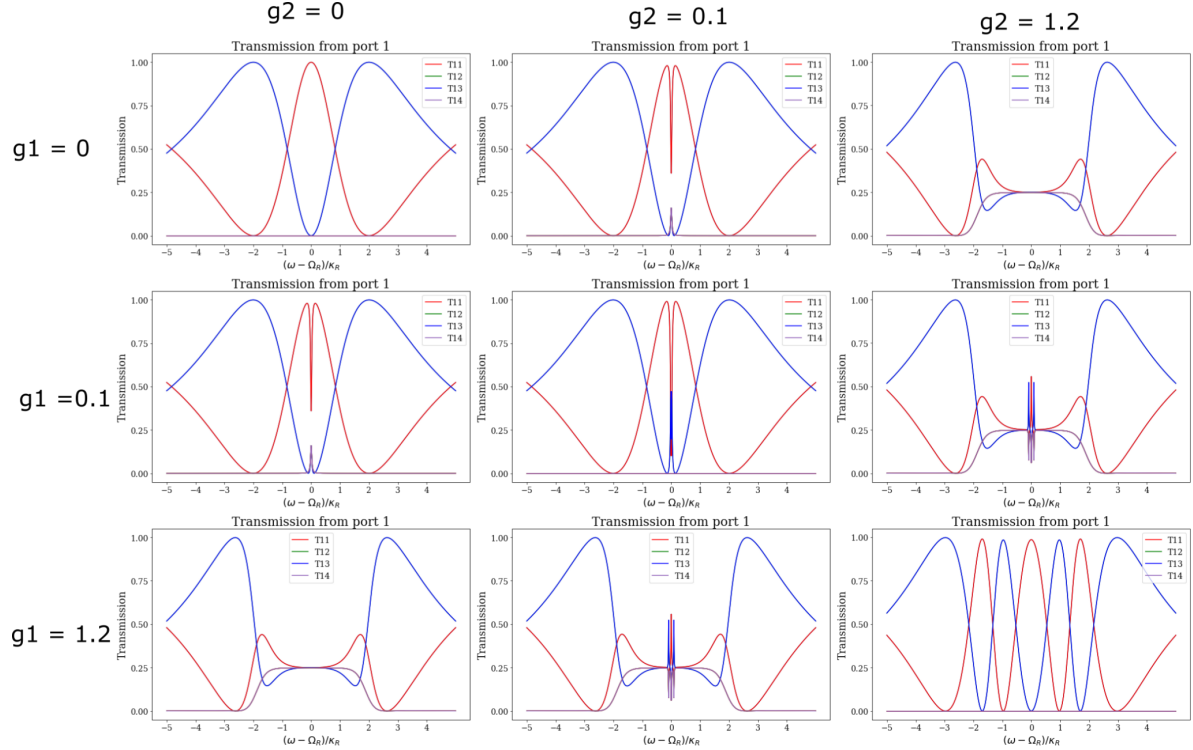


Figure 19.1: Model 2 ZZ transmission probabilities with the photon input at port 1 and the emitters on-resonance with the cavity frequencies for both Z systems, at various coupling strengths between odd and even modes of the cavity and the pair of emitters.

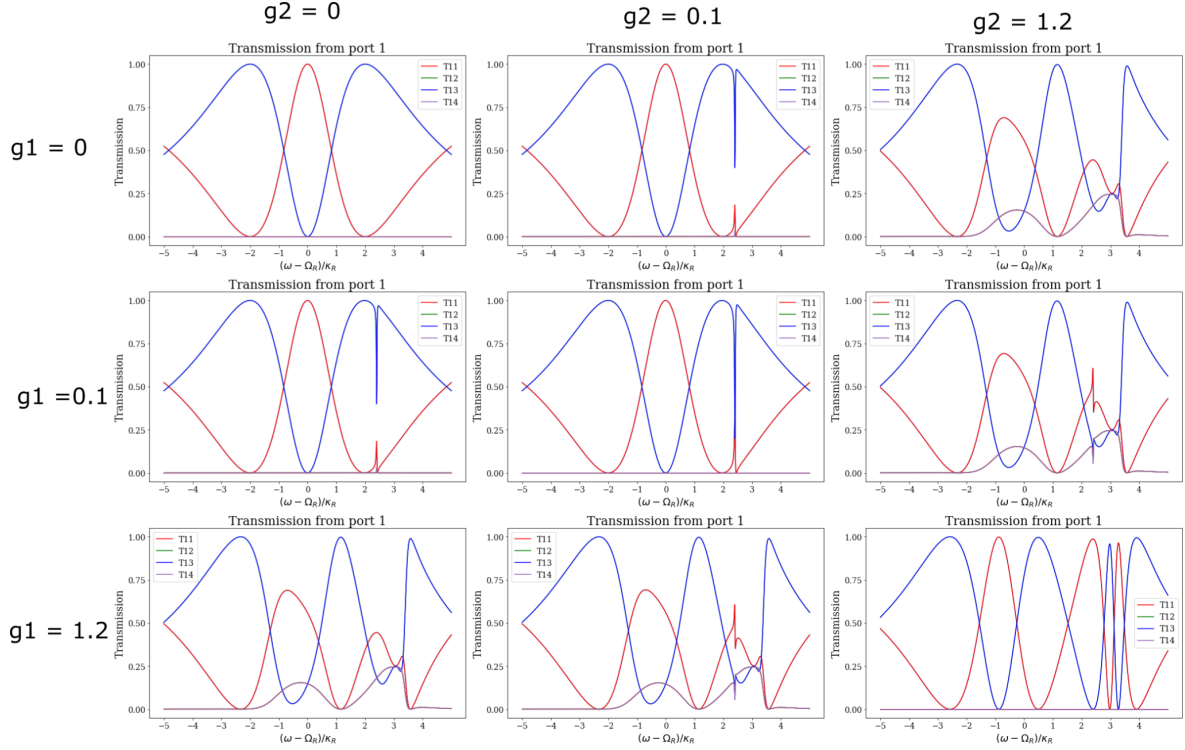


Figure 19.2: Model 2 ZZ transmission probabilities with the photon input at port 1 and the emitters off-resonance with the cavity frequencies for both Z systems, at various coupling strengths between odd and even modes of the cavity and the pair of emitters.

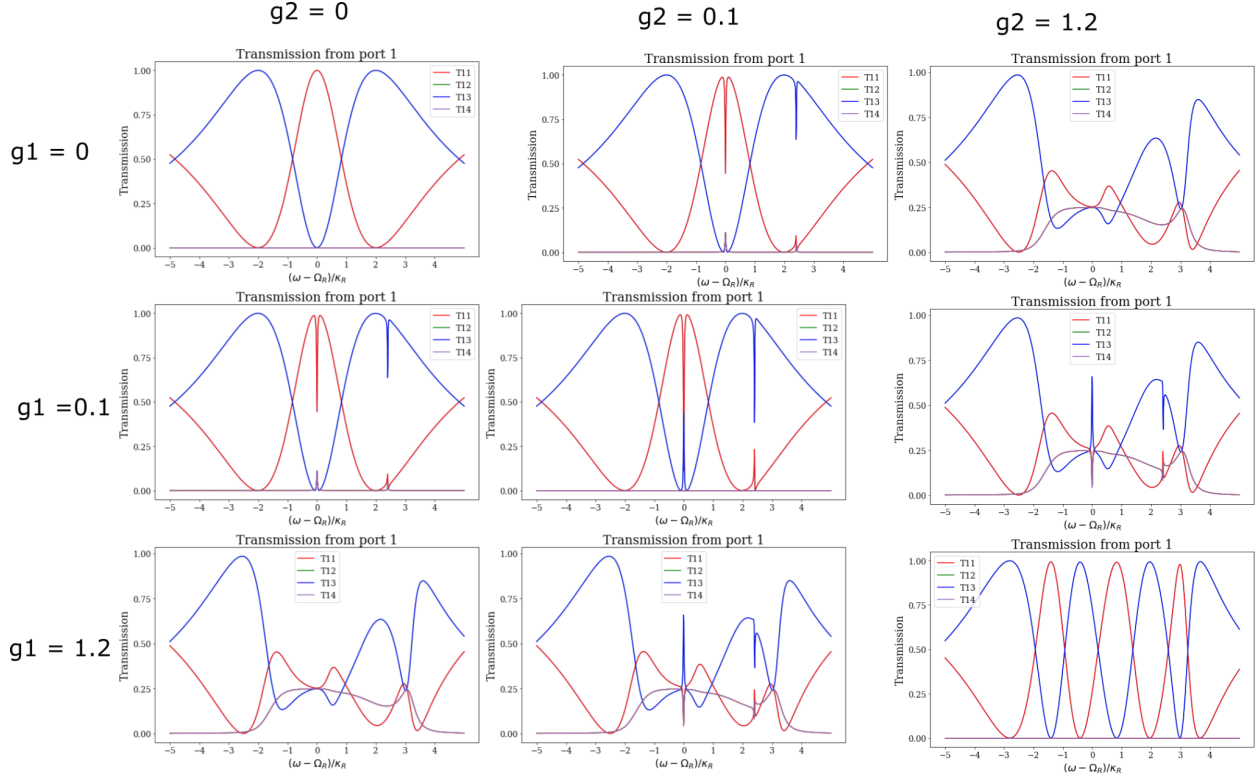


Figure 19.3: Model 2 ZZ transmission probabilities with the photon input at port 1, the emitters of the first Z system on-resonance, and the emitters of the second Z system off-resonance with the cavity frequencies for both Z systems, at various coupling strengths between odd and even modes of the cavity and the pair of emitters. The behaviour is the same if we make the first Z system off-resonance and the second on-resonance instead.

Monte Carlo Simulation

Finally, we chose an operating point and simulated ten Model 2 systems with parameters normally distributed around said operating point. The simulated values are tabulated in Table 2. Meanwhile, we see the results in Figure 20 for both the Z and ZZ systems. We note that, for an off-resonance emitter detuning of 2.4 (normalised), a coupling coefficient of 0.5 for each emitter strikes a reasonable balance between the width of the transmission peaks with respect to photon detuning, and the transmission at the off-resonance detuning. Nonetheless, the ZZ system transmission peaks in particular are very narrow in frequency (a better system would have a greater emitter detuning and greater coupling between modes and the emitters). The desired transmission and reflection peaks, despite the normal errors added to the system, remain fairly well-defined.

Parameter	Set in software with:	Mean	Standard Deviation	Description
ω_{emit}	dw_emit_ref	0 (on-resonance) 2.4 (off-resonance)	0.05	Emitter detuning from the reference (normalized).
ω_{even}	dw_mode_ref	0	0.05	Even mode detuning from the reference
ω_{odd}	dw_mode_ref	0	0.05	Odd mode detuning from the reference (normalized)
g_{even}, g_{odd}	g_mode_emit	0.5	0.05	Coupling between both the even and odd cavity modes and the emitter
$\Gamma_{even}, \Gamma_{odd}$	mode_loss	0	0	Loss from the even and odd cavity modes
γ	emit_loss	0	0	Losses from the emitter
$\kappa_{f, even}$	waveguide_coupling_mu ltiplier waveguide_coupling	$\frac{1}{\sqrt{2}} [1 1 1 1]$	0.05 per entry	Coupling of the fields (not the power) between the even mode and each waveguide. The elements of the vector are given as port 1, port 2, port 3, port 4
$\kappa_{f, odd}$	waveguide_coupling_mu ltiplier waveguide_coupling	$\frac{1}{\sqrt{2}} [1 -1 1 -1]$	0.05 per entry	Coupling of the fields (not the power) between the odd mode and each waveguide

Table 2: Mean and standard deviation of parameters for Model 2 Monte Carlo simulation

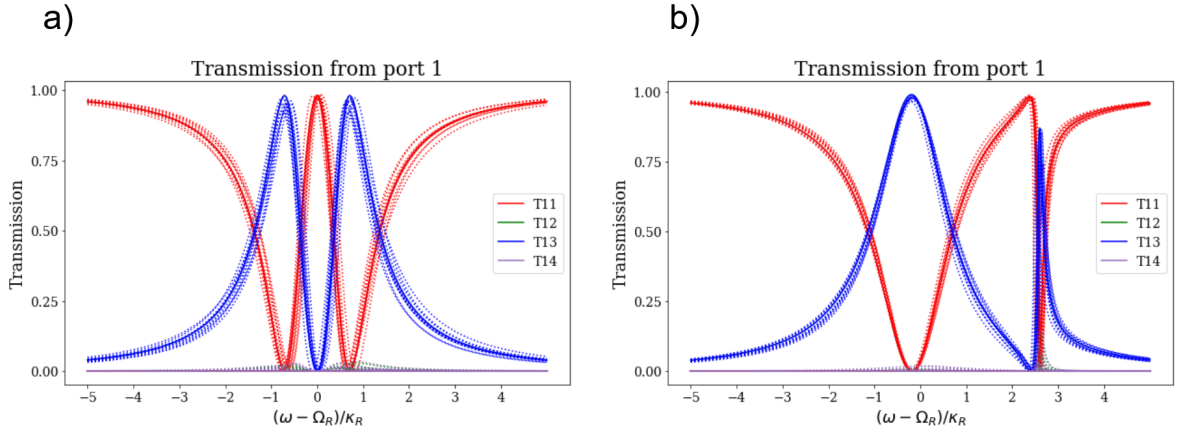


Figure 20: Monte Carlo simulation of Z system transmission for on-resonance emitters (a) and off-resonance emitters (b), around a given setpoint (see Table 2). Errors on each parameters are on the order of $0.05\kappa_R$.

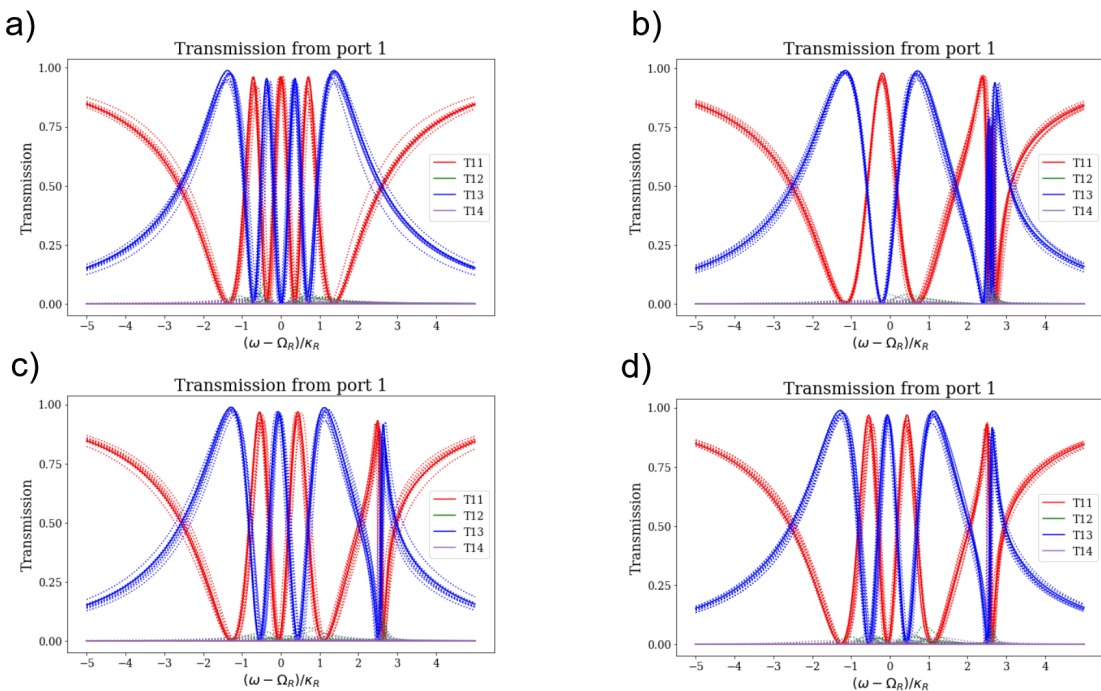


Figure 21: Monte Carlo simulation of ZZ system transmission for on-resonance emitters in both Z systems (a), off-resonance emitters in both Z systems (b), on-resonance emitters in the first Z system and off-resonance emitters in the second Z system (c), and off-resonance emitters in the first Z system and on-resonance emitters in the second Z system. Monte Carlo sweep is taken around a given setpoint (see Table 2). Errors on each parameters are on the order of $0.05\kappa_R$.

ZZ System Error Metrics

The cascaded inner product is now swept over waveguide-cavity coupling strength and system loss for the ZZ system in Figure 22. Once again, the particular system parameters has $\kappa_{i,j} = \pm\kappa/\sqrt{2}$ and loss rate of Γ for all cavity modes and emitters. For symmetry, both Z halves of the ZZ system are constrained to have the same parameters in these sweeps.

From Figure 22, we again see that emitter-cavity coupling ($g = 1$ for all emitters) is necessary for ideal operation. However, the emitter-coupled ZZ system appears to be less robust to loss than the Z system, exhibiting a significant departure from optimal behaviour on the scale of $\Gamma \sim 0.05$. Meanwhile, when one or both of the emitters a Z half is decoupled, the performance again quickly deteriorates with just a bit of loss. And again, moderate cavity-waveguide coupling ($\kappa \sim 1$) is ideal when the emitters are coupled.

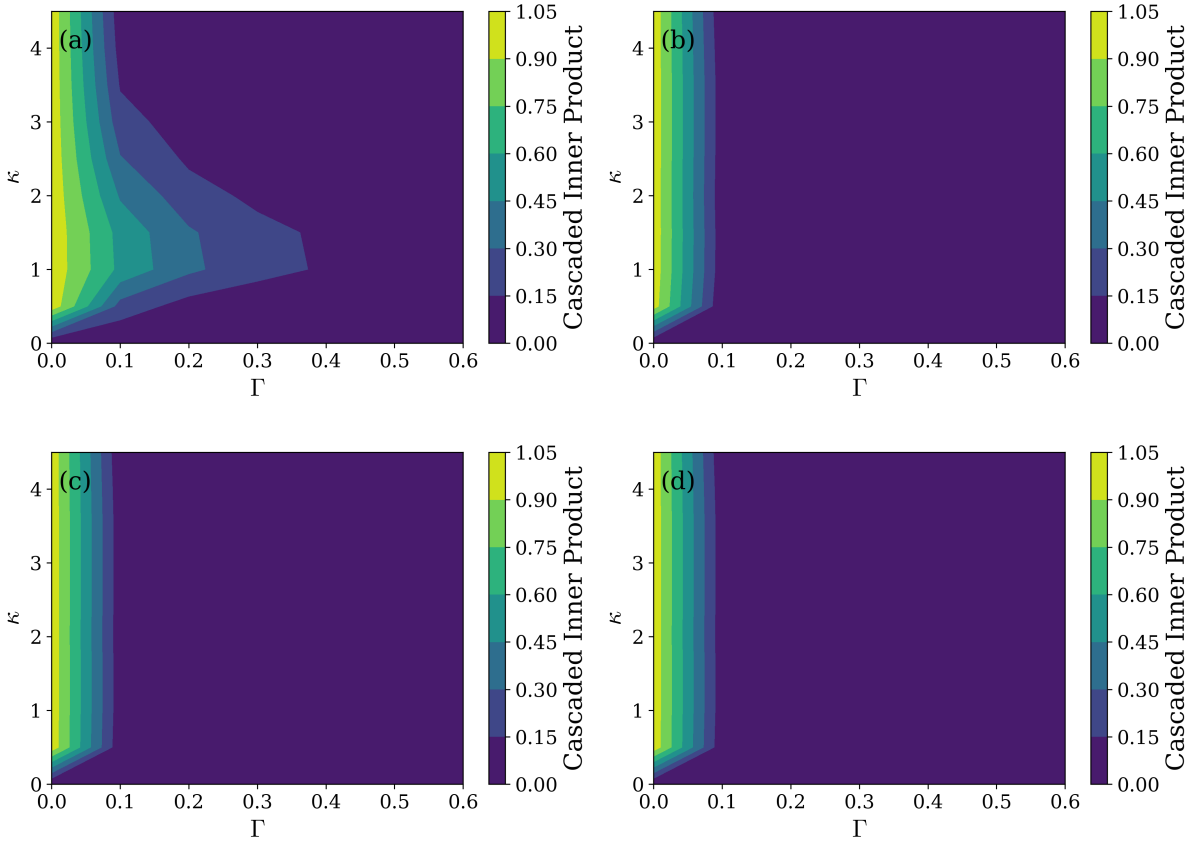


Figure 22: Error metric sweeps over cavity-waveguide coupling strengths and system loss for the ZZ system, with symmetrically-parametrized Z halves. This is presented for various emitter-cavity mode coupling strengths: (a) $g_1 = g_2 = 1$, (b) $g_1 = 1, g_2 = 0$, (c) $g_1 = 0, g_2 = 1$, (d) $g_1 = g_2 = 0$. The units are normalized as discussed previously. Finally, the metrics are combined over all frequencies using a maximization rule.

Dual-Emitter Conclusions

We find that Model 2 allows us to build a symmetric system with the desired switching behaviour controlled by on and off-resonance emitters. We also qualitatively see that, unlike in Model 1 where significantly different couplings between the odd and even mode seemed to stop the switching behaviour entirely, Model 2 seems to maintain a small transmission peak near $\omega = 0$ even when g_1, g_2 were very different. Other significant points were:

1. The transmission peak width with respect to photon detuning narrowed in ZZ systems. When engineering these cavity systems, the design should be made with the ZZ sensitivity (rather than the Z sensitivity) in mind.
2. Large cavity coupling
3. In engineering these systems, we would in general suggest aiming for the largest possible off-resonance detuning achievable, and then to subsequently sweep over coupling strengths using our error metric utilities in order to pick the best balance between wide transmission peaks with respect to photon detuning (high cooperativity), and the off-resonance emitters sufficiently switching the peak.
4. The presence of emitter-cavity coupling is still required for ideal behaviour.
5. Optimal system parameters again include moderate cavity-waveguide coupling ($\kappa \sim 1$) and no loss.
6. The ZZ system is less robust to photon loss than the Z system in terms of error performance.

Inherent in this model is the assumption that the two emitters of the system act together as a single logical qubit. That is, we assume that two emitters will always be in the same state or superpositions of state. Whether or not the emitters are likely to detune with respect to each other still has to be investigated.

Model 2B: Dual-Cavity, Dual-Emitter ZZ System

Our Jupyter notebook also proposes a 2-cavity single Z system which has similar behaviour to this Model 2 Z system candidate. This would allow us to obtain similar behaviour without having to design cavity systems with multiple modes (then, each cavity would need only one mode, where the odd and even modes in the system as a whole would come from the superposition of the modes of each cavity). A more detailed analysis of this system and the differences between the two topologies is in Appendix B: Model 2B.

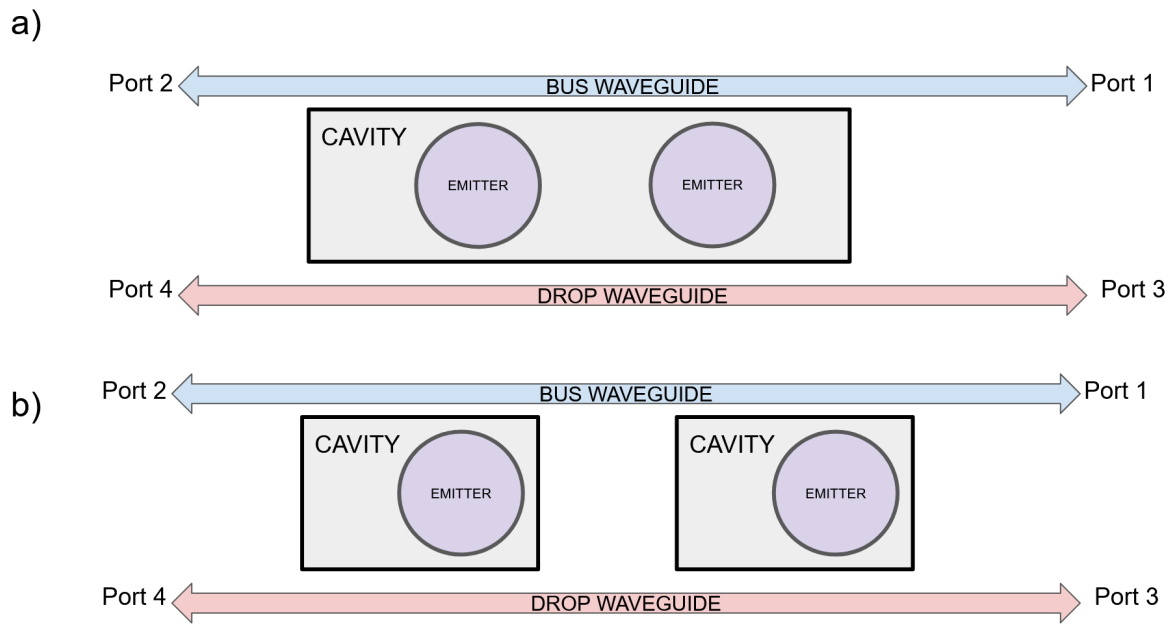


Figure 23. A similar topology to the one simulated, seen again in a) is a two cavity implementation b) in this topology two separate but identical cavities supporting a single mode and single emitter are placed next to each other. The even and odd components of the system are formed from even and odd superpositions of the two cavity subsystems.

Conclusion

In terms of the system structure, we found that a single-emitter system cannot simultaneously exhibit nontrivial odd and even emitter-mode coupling symmetry. This led us to develop dual-emitter Z and ZZ systems, where these desired symmetries are present. A second finding in the system architecture is that directional port behaviour can be physically controlled by manipulating phases, although more work needs to be done to elucidate this.

As for performance, a high cooperativity factor negatively impacts the system's transmission switching behaviour and requires increased emitter detuning to compensate. Elsewhere, the systems have been found to behave poorly with low emitter-cavity coupling. Holding this constant, moderate waveguide-cavity coupling and low photon losses result in ideal performance.

Recommended metrics for performance evaluation are fidelity and the cascaded inner product, which is a generalization of p_{max} . These two metrics produce similar results. Meanwhile, error metrics such as trace distance and relative entropy are advised against.

These results have been arrived at from a combination of analytical improvements to previous work, development of numerical code to perform computations, and communication with sponsors to clarify priorities and potential issues. Since the results have been validated through a conjunction of unit testing, analytical sanity-checking, and replication of past work, the primary risks associated with the findings arise from the various assumptions built into the models and dynamics analysis—these are outlined in further detail in *Appendix B*.

Recommendations

We recommend designing for the ZZ system rather than the Z system because the former is the weakest link in terms of error propagation. This is because the ZZ system is more sensitive to photon detuning and less robust to photon loss. The design parameters for the ZZ system should include nonzero emitter-cavity coupling, moderate cavity-waveguide coupling, and low photon loss, as these have been found to result in optimal performance. Although the sweeps in this report have been performed for reasonable configurations (i.e. other parameters), the particular ideal values are subject to change in these details and can be obtained using the software package we have developed. To this end, we recommend using the cascaded inner product or fidelity metric to evaluate potential designs.

Future Work

We recommend these follow-ups to the work done in this report:

1. **Investigate the effect of phase shifts in coupling coefficients** (e.g. waveguide-to-mode coupling as well as mode-to-emitter coupling). We saw in Model 1, for example, that phase shifts in these coefficients can control the directionality of the system—it is therefore important to understand the effects of these phase shifts (and of phase errors) on the system.
2. **Investigation of other resonator systems.** We investigated photonic crystal cavities in this report; our analysis could be ported to the study of scattering against ring resonators and the corresponding alternate implementations.
3. **Investigate whether two emitters can act as an effective qubit.** In Model 2, we assume that we can have two emitters in the system act together as a single qubit (always having the same state). This assumption requires further investigation.
4. **Investigate stability of models 1 and 2 with respect to mode-emitter coupling.** Our preliminary sweep indicated that system performance deteriorates when the coupling coefficient between emitters and the odd and even modes change. However, our sweep was quite coarse. We would recommend investigating smaller differences in coupling coefficients.
5. **Extend our analysis to higher excitation subspaces.** This would allow us to predict system behaviour when multiple photons are input.
6. **Connect the general figures of merit for error to specific error-correcting codes.** This would provide a more refined evaluation of potential system designs when a particular scheme for error correction has been chosen.

Deliverables

The deliverables for this project include:

1. Sweep results of transmission probabilities and error metrics for the Z and ZZ systems
2. A software package that solves the dynamics, computes transmission probabilities and error metrics, and performs sweeps over specified ranges of parameters
3. A report documenting the analysis and results obtained
4. Jupyter notebook tutorials outlining how our software package can be used

Appendix A: Testing and Validation

Testing and validation has relied on the following:

1. Software unit tests (implementing sanity checks and other validation)
2. Symmetry analysis sanity checks
3. Replicating previous results (from Sebastian Gitt's thesis)

Unit Tests

These tests can be found under cavityQED_dynamics/testing. They include:

1. **unitarity_test.py**: this set of tests checked that lossless S matrices gave us unitary matrices and that S matrices with loss terms did not give us unitary matrices.
2. **test_metrics.py**: confirms that error metric implementations give desired results
3. **test_waggs.py**: confirms that frequency aggregation implementations give desired results

Symmetry Checks

We explained results we found computationally with symmetry analysis—this analysis was included in the body of the report, and provided us with confidence that our simulations were physically based.

Reproducing Previous Results

A Jupyter Notebook replicating Sebastian's results can be found under:

`cavityQED_dynamics/testing/thesis_sweeps_replication.ipynb`

This notebook confirms that our software framework (implemented to support an arbitrary number of ports, emitters, and cavity modes) can retrieve the 2 ports, 1 emitter, 1 cavity results presented in Sebastian's thesis. It demonstrates that we can replicate the following:

1. The transmission behaviour of an empty cavity
2. The transmission pattern at different cooperativities
3. The transmission patterns at different emitter detunings
4. The increasingly broad splitting which occurs as we increase the number of emitters in the cavity

Appendix B: Hamiltonian, Symmetry Analysis,

and Theory for Models

Model 1

The hamiltonian for this system is given by:

$$H_{\text{eff}} = \left(\omega_\sigma - i \frac{\gamma}{2} \right) \sigma^\dagger \sigma + \left(\omega_{\text{odd}} - i \frac{\Gamma_{\text{odd}}}{2} \right) a_{\text{odd}}^\dagger a_{\text{odd}} - g_{\text{odd}} (\sigma a_{\text{odd}}^\dagger + a_{\text{odd}} \sigma^\dagger) \\ + \left(\omega_{\text{even}} - i \frac{\Gamma_{\text{even}}}{2} \right) a_{\text{even}}^\dagger a_{\text{even}} - g_{\text{even}} (\sigma a_{\text{even}}^\dagger + a_{\text{even}} \sigma^\dagger) - \frac{i}{2} \sum_l L_l L_l^\dagger$$

It's matrix form it can be given as:

$$H_{\text{eff}} = \begin{bmatrix} \omega_\sigma - i \frac{\gamma}{2} & -g_{\text{even}} & -g_{\text{odd}} \\ -g_{\text{even}} & \omega_{\text{even}} - i \frac{\Gamma_{\text{even}}}{2} & 0 \\ -g_{\text{odd}} & 0 & \omega_{\text{odd}} - i \frac{\Gamma_{\text{odd}}}{2} \end{bmatrix} - \frac{i}{2} \begin{bmatrix} 0 & 0 & 0 \\ 0 & \|\kappa_{\text{even}}\|^2 & \kappa_{\text{even}} \cdot \kappa_{\text{odd}}^* \\ 0 & \kappa_{\text{odd}} \cdot \kappa_{\text{even}}^* & \|\kappa_{\text{odd}}\|^2 \end{bmatrix}$$

A requirement for symmetrical, ideal behaviour of the cavity-emitter system is that it can be block diagonalize into a form:

$$H_{\text{eff}} = \begin{bmatrix} H_{\text{even}} & \\ & H_{\text{odd}} \end{bmatrix}$$

This holds if the system is symmetric along the X and Y axis. However it can be shown that this symmetry cannot hold if both the odd and even cavity modes are coupled to the emitter. The simple explanation for this is that the odd mode has zero amplitude on the y axis. And so if we place the emitter there, the odd mode cannot couple.

Therefore the only way we can construct a system where both the odd and even modes couple to the emitter is to place the emitter off of the y-axis. This introduces an asymmetry to the system which causes different behaviour depending on which direction the photon is input. This is because the relative phase of the odd and even mode, will flip depending on which direction the photon enters from. If we suppose for a photon

input from one direction the odd and even mode destructively interfere over the emitter, then the cavity-system will behave as if there is no emitter. A photon input from the other direction will necessarily cause the odd and even modes to constructively interfere, and so the cavity will behave as if the emitter is present.

To control the behaviour of this system therefore requires engineering the relative phase of the even and odd coupling to the waveguide.

Model 2

The Hamiltonian for this system is given by:

$$H_{\text{eff}} = \sum_{i \in \{1, 2\}} \left[\left(\omega_{\sigma_i} - i \frac{\gamma_i}{2} \right) \sigma_i^\dagger \sigma_i + \sum_{j \in \{\text{even}\}} \left[\left(\omega_j - i \frac{\Gamma_j}{2} \right) a_j^\dagger a_j - g_j (\sigma_i a_j^\dagger + a_j \sigma_i^\dagger) \right] \right] - \frac{i}{2} \sum_l L_l L_l^\dagger$$

The matrix form of this Hamiltonian can be written:

$$H_{\text{eff}} = \begin{bmatrix} \omega_{\sigma_1} - i \frac{\gamma_1}{2} & 0 & -g_{1,\text{even}} & -g_{1,\text{odd}} \\ 0 & \omega_{\sigma_2} - i \frac{\gamma_2}{2} & -g_{2,\text{even}} & -g_{2,\text{odd}} \\ -g_{1,\text{even}} & -g_{2,\text{even}} & \omega_{\text{even}} - i \frac{\Gamma_{\text{even}}}{2} & 0 \\ -g_{1,\text{odd}} & -g_{2,\text{odd}} & 0 & \omega_{\text{odd}} - i \frac{\Gamma_{\text{odd}}}{2} \end{bmatrix} - \frac{i}{2} \begin{bmatrix} 0 & 0 & 0 & 0 \\ 0 & 0 & 0 & 0 \\ 0 & 0 & \|\kappa_{\text{even}}\|^2 & \kappa_{\text{even}} \cdot \kappa_{\text{odd}}^* \\ 0 & 0 & \kappa_{\text{odd}} \cdot \kappa_{\text{even}}^* & \|\kappa_{\text{odd}}\|^2 \end{bmatrix}$$

A requirement for symmetric ideal behaviour of the cavity scatterer is that the Hamiltonian can be block diagonalized in the form:

$$H_{\text{eff}} = \begin{bmatrix} H_{\text{even}} & \\ & H_{\text{odd}} \end{bmatrix}$$

Enforcing mirror symmetry in the X and Y axis is enough to achieve this block diagonalization and unlike in Model 1 this can be done without placing the emitters on a node of the odd cavity mode. In this system both modes are coupled to the two emitters, however due to their symmetry the relative phase of the coupling to each emitter can be enforced as:

$$g_{1,\text{even}} = g_{2,\text{even}}, \quad g_{1,\text{odd}} = -g_{2,\text{odd}}$$

In addition if the emitters are identical, and the waveguide symmetry holds then we also have:

$$\kappa_{\text{even}} \cdot \kappa_{\text{odd}}^* = 0, \quad \omega_{\sigma_1} = \omega_{\sigma_2}, \quad \gamma_1 = \gamma_2,$$

These constraints guarantee unity transmission if the cavity, emitter and photon frequencies are resonant, they are also guaranteed by physical symmetry. Any analysis of the sensitivity of this topology should begin from these parameters.

Model 2B

A similar topology to the one analyzed is a two cavity implementation as in Figure 23 In this topology two separate but identical cavities supporting a single mode and single emitter are placed next to each other. The hamiltonian for this system can be written as:

$$H_{\text{eff}} = \sum_{i \in \mathbb{Z}_2} \left[\omega_e^{(i)} \sigma_i \sigma_i^\dagger + \omega_c^{(i)} a_i a_i^\dagger + g_i a_i \sigma_i^\dagger + g_i^* \sigma_i a_i^\dagger \right] + \Lambda a_1 a_2^\dagger + \Lambda^* a_2 a_1^\dagger - \frac{i}{2} \sum_l L_l L_l^\dagger$$

Here H is the sum of the two single emitter, single mode hamiltonians, where we have allowed some coupling between the cavities through the lattice governed by the coupling constant Λ . It can be shown that if the cavities are identical and we take the even and odd superposition of the cavity and emitter modes, this system can be written as:

$$H_{\text{eff}} = \sum_{i \in \{\text{even, odd}\}} \left[\omega_e \sigma_i \sigma_i^\dagger + (\omega_c \pm \Lambda) a_i a_i^\dagger + g a_i \sigma_i^\dagger + g^* \sigma_i a_i^\dagger \right] - \frac{i}{2} \sum_l L_l L_l^\dagger$$

A difference between this system and the single cavity 2 emitter topology, is that the inter-cavity coupling governed by Λ causes the even and odd mode frequencies to split. Since we require that both the even and the odd cavity modes be resonant with the even and odd emitter modes this inter-cavity coupling is undesirable, and the cavities should be placed sufficiently far apart that there is no coupling through the lattice. An additional difference is that the mode-emitter coupling g is guaranteed by symmetry to be identical which may have advantages.

There is one more important constraint that must be applied to ensure ideal behaviour of this system. Because the cavities are separated, an incoming photon will encounter the second cavity at a relative phase offset from the first cavity. This manifests in a difference in phase of the coupling constant κ between a

waveguide and the first cavity vs the second cavity. If the second cavity is in phase with the first cavity, then only the even mode is excited and we get no excitation of the odd mode. Conversely if the first cavity is in the opposite phase with the second cavity, then only the odd mode is excited. Therefore to excite both even and odd components equally the phase angle should be set to $\pm\pi/2$, and the displacement of the cavities should be:

$$d = \frac{\lambda}{4}(2n + 1)$$

Where λ is the wavelength of the incoming photon. This is consistent with the discussion in (Fan 1998a). The coupling coefficients can be given by:

$$\kappa_{l,1} = (\kappa \quad \kappa e^{i\frac{2\pi}{\lambda}d} \quad \kappa \quad \kappa e^{i\frac{2\pi}{\lambda}d}), \quad \kappa_{l,2} = (\kappa e^{i\frac{2\pi}{\lambda}d} \quad \kappa \quad \kappa e^{i\frac{2\pi}{\lambda}d} \quad \kappa)$$

Where we have taken the first and third entries of the coupling vector as representing the rightward travelling modes, and the second and fourth entries as representing leftward travelling modes.

Appendix C: Software Package

The analysis above was facilitated by a software which we wrote in Python. More in-depth documentation is provided in the package itself. The following is a high-level summary of the software components.

Summary of Classes

cQEDSystem_LPorts_Mmode_Nemit

This is our implementation of a **cQEDSystemInterface** class (though the software is designed such that other system representations could be implemented). This class:

- Saves the system description (e.g. frequencies of operation, frequency detuning, losses, coupling coefficients) including the mean and predicted standard deviations of system parameters (these values can be estimated from manufacturing tolerances)
- Can produce normally distributed sample parameters according to the means and standard deviations defined, to allow analysis of the robustness of systems

Hamiltonian_Mmodes_Nemit

This is once again our only implementation of the **HamiltonianInterface**, though any implementation with the same API would be accepted by the code base. This class:

- Creates a lambda function for calculating the single-excitation effective Hamiltonian of the system from the parameters contained in **cQEDSystem_LPorts_Mmode_Nemit**.
- Returns the numerical effective Hamiltonian
- Diagonalizes the numerical effective Hamiltonian (something which our dynamics calculations require)

ErrorMetric

These classes are used to evaluate the all-states error metric over an array of photon frequencies. The inputs are:

- **basis:** the ideal behaviour corresponding to each basis
- **S_all:** first-row S matrix elements for at each photon frequency

The error metric returns the metric value at each photon frequency. The implemented error metrics are:

- Cascaded inner product
- Fidelity
- Trace distance

WAggregate

This class aggregates error metrics over a range of photon frequencies into a single figure of merit. The inputs are:

- **w**: photon frequencies over which the error metric has been computed
- **mvals**: the corresponding metric values

An aggregation returns a single real number that represents an overall figure of merit. The implemented aggregation schemes are:

- Maximization
- Minimization
- Integration
- Bandwidth

DynamicsSolverLPort

Our implementation of the **DynamicsSolverInterface**. This class:

- Generates S-matrices of a system over a range of photon detuning from the reference, given a **cQEDSystemInterface** and **HamiltonianInterface** object.
- Can concatenate 2 matrices (if they are both invertible) to model sequential cavity systems (e.g. combine Z system S-matrices into a ZZ system S-matrix)
- Provides transmissions at each port when given the computed S-matrix

Additional Utilities

We also provide various utilities to facilitate the process of sweeping and plotting parameters.

param_sweep.py

- A Monte Carlo function to generate S-matrices, transmission results, and error metric results over expected errors in all parameters (uses the normal distribution sampling from the `cQEDSystemInterface` classes)
- A line sweep function over a single parameter, where the S-matrices, transmission results, and error metrics are returned for each value of the given parameter
- A grid sweep function over pairs of parameters, where the S-matrices, transmission results, and error metrics are returned for each pair of values of the given parameters
- Some additional functions to help set up sweeps (see Jupyter notebook example sweeps for further details)

plot_utils.py

- A function to plot transmission with a consistent layout and colour scheme

The docstrings for the classes provide further information on the API. Our example and sweep Jupyter notebooks can be used as examples.

Workflow

The workflow to simulate a system, or to sweep parameters of a system can be seen in our Jupyter notebooks.

Appendix D: Background Theory

Input output Model

The first step in the scattering analysis is to derive an energy conservation law governing how energy enters and exits the system. We do this by introducing creation operators.

$$b_{\omega,l}(t), \quad a_r(t), \quad L_l(t) = \sum_r \kappa_{lr} a_r(t)$$

Where b_l is an annihilation operator acting on port l at frequency ω , a_r is an annihilation operator acting on a photon mode in the cavity. And L_l is an operator representing the coupling between the cavity photonic modes and the waveguides. The coefficients κ_{lr} are coupling coefficients, calculated from the overlap of the photonic cavity mode profiles and the waveguide mode profiles. Using these operators and a Hamiltonian description of the system it can be shown that:

$$b_{\text{out}}^{(l)}(t) = b_{\text{in}}^{(l)}(t) - i \sum_l L_l(t)$$

Where $b_{\text{out}}^{(l)}$ and $b_{\text{in}}^{(l)}$ are “field” operators representing the field near the scatterer as a function of time. An accessible derivation of these equations is found in (Combes, 2017). These “input output equations” hold for each waveguide and are important because they relate the dynamics of the waveguides to the dynamics of the cavity-mode operators $a_r(t)$.

Scattering Matrices

In quantum mechanics the time evolution of a state is given by a unitary time evolution operator calculated from the Hamiltonian of the system written:

$$U(t_0, t) |\psi(t_0)\rangle = |\psi(t)\rangle$$

The probability amplitude of transition from one state to another in the time t is given by:

$$\langle \psi_2(t) | U(t_0, t) | \psi_1(t_0) \rangle$$

The elements of the scattering matrix can then be written:

$$S_{ij} = \lim_{\substack{t \rightarrow \infty, \\ t_0 \rightarrow -\infty}} \langle \psi_j(t) | U(t_0, t) | \psi_i(t_0) \rangle$$

If the system has a finite number of states then we can represent $U(t_0, t)$ (and S) as a finite matrix. Unfortunately, the waveguides in our system can hold a continuum of states and to account for all of them is not computationally tractable. However if we restrict the cavity-emitter system to a single photonic excitation, we can write the cavity-emitter evolution in terms of a finite matrix. This is where the input-output equations enter, using them we can describe the evolution of the input and output states of the system in terms of the cavity-mode evolution. It can be shown that the S matrix as a function of input photon frequency can be written:

$$S_{ij}(\omega) = i \sum_{r,l \in \mathbb{Z}_M^2} \kappa_{jl} \kappa_{ir}^* \mathcal{G}_{rl} + \delta_{ij}$$

Where M is the number of photonic cavity modes that couple to the waveguides, δ_{ij} is a kronecker delta function, and G is a finite matrix written:

$$\mathcal{G} = V \mathcal{D} \left\{ \frac{1}{\lambda^{(1)} - \omega} \right\} V^\dagger$$

The vector λ is a vector of eigenvalues of the Hamiltonian of the single photon cavity-emitter system, the D $\{\frac{1}{\lambda - \omega}\}$ is a diagonal matrix formed from this vector. The matrix V is a matrix of eigenvectors of the Hamiltonian.

Since the Hamiltonian is of the finite basis single-photon cavity-emitter system it can be written as a finite matrix depending on the system of interest.

S and M matrices

To construct the concatenated ZZ scattering matrix can be done in a highly straight forward-using M matrix. If we consider the S matrix as the matrix that maps input to output

$$S : \text{Input} \rightarrow \text{Output}$$

Then M matrices are the matrix that maps left to right.

$$M : \text{Left} \rightarrow \text{Right}$$

M matrices can be concatenated by multiplying so:

$$M_{ZZ} = M_1 M_2$$

M matrices are constructed by taking a partial inverse of the S matrix. If we call this partial inverse operation P_{inv} then we have:

$$P_{\text{inv}}(S) = M$$

$$S_{ZZ} = P_{\text{inv}}(P_{\text{inv}}(S_1)P_{\text{inv}}(S_2))$$

This is the approach to studying the ZZ hamiltonian that we take in this report. Although in principle a full Hamiltonian could be constructed for the ZZ system and there may be some advantages to doing so.

Error Metrics

Various sources of real-world error deviate the systems' behaviours from ideal operation. One particular case is when a photon is lost from the cavity or waveguides to the external environment. This is modelled in the Hamiltonian as memoryless loss rates in the form of $i\gamma a^\dagger$ terms, where γ is a loss rate and a^\dagger is a creation of the photon in the location where it is lost from. Under Heisenberg evolution, this yields an exponential decay term:

$$\dot{a}^\dagger = \dots - \gamma a^\dagger$$

The characterization of loss as a memoryless rate is reasonable in light of Fermi's golden rule. This is particularly true because the environment is much larger than the system, so that the occurrence of undesirable “gains” from photons leaking in is negligible (presumably, any source of systematic external radiation, such as a powerful lightbulb in the room, will be removed or screened appropriately in the physical setup).

Roughly speaking, the no-loss time-dependent creation/annihilation operators are thus masked by an exponential decay envelope owing to all the losses. Although, the particular transient amplitudes of the operators are likely more complicated due to the coupled interactions between the various degrees of freedom in these systems, the qualitative behaviour of decayed dynamics still holds.

Let $a(t)$ be a time-dependent operator for a lossy system, with $a_0(t)$ being the corresponding operator in a lossless system. For simplicity, the lossless system is a 1-emitter 2-mode Z system with a homogeneous loss rate of γ for its two cavity modes and emitter. Then this discussion suggests:

$$a(t) \approx a_0(t)e^{-\gamma t}$$

Note that this is an overestimate of the loss as there is no loss from the waveguide modes despite them containing a nonzero component of the photon's quantum state. When the operators are ultimately Fourier transformed in the S matrix elements to obtain transmission probabilities, the convolution theorem applies. That is, the lossy transmission probabilities are a convolution, in photon frequency, of the lossless transmission and the Fourier transform of $e^{-\gamma t}$. Extending the exponential decay to be two-sided for the Fourier transform, the latter Fourier transform is simply a Lorentzian. Thus,

$$T_{loss}(\omega) \approx \frac{1}{2\pi} \int_{-\infty}^{+\infty} d\omega T_{no-loss}(\omega) \frac{2\gamma}{\omega^2 + \gamma^2}$$

This rough analysis is confirmed in Figure D.1 when comparing a lossy bus transmission rate with its convolutional prediction for a spin-up qubit with $\gamma = 0.01$. As can be seen, the lossy transmission probabilities near $\omega = 0$ are indeed smaller than the no-loss counterpart. Furthermore, the predicted lossy transmission from convolution matches the actual lossy transmission profile quite well, considering the presence of minute discrepancies due to no waveguide loss and non-trivial interactions between the degrees of freedom (probabilities away from $\omega = 0$ are inaccurate in Figure D.1 due to truncation of the convolution integral as the domain limits are breached).

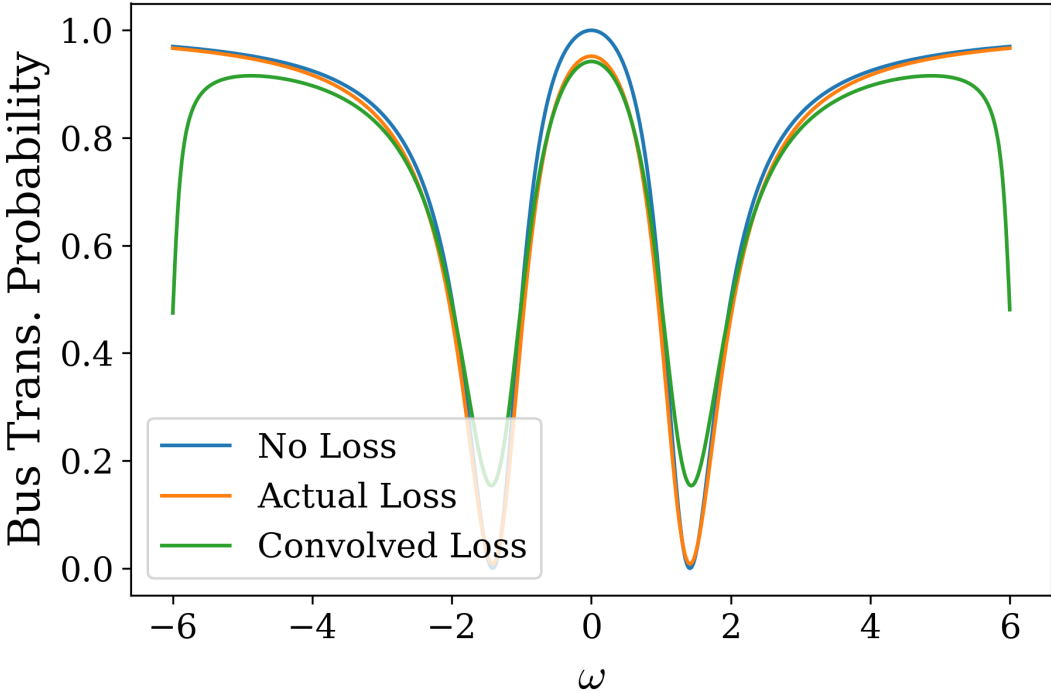


Figure D.1: Comparison of the actual loss transmission and predicted convolutional loss transmission for a 2-mode 1-emitter spin-up Z system. The no loss transmission probability profile is plotted for reference. Both cavity modes, as well as the emitter, exhibit a loss rate of 0.01. The abscissa ω represents the normalized photon frequency relative to the cavity's resonant frequency; the normalization of units are described later in this document. The convolutional prediction for larger $|\omega|$ is inaccurate due to cutoff from integrating over a finite ω domain.

This analysis suggests that photon loss effects are incorporated implicitly in the S matrix formalism. Furthermore, the nature of photon loss is accurately understood as resulting in a deterioration of transmission probabilities. The only type of error to account for, then, is the difference in actual transmission probabilities from the desired ones. This includes both photon loss issues as well as shortcomings in the various parameters that define a particular system design.

Beyond photon loss, the only possibly measurable events are when the photon exits one of the ports. For the Z system, backreflections (i.e. exits through the backwards ports) are erroneous as their presence decreases the likelihood of bus or drop transmission. Therefore, the impact of backreflections is also accounted for by considering only forward transmission probabilities. For the case of a two-cavity ZZ system, backreflections in the left half are similarly accounted for, leaving only backreflections in between cavities problematic. These are, however, accounted for in the SM-matrix algebra; a full-Hamiltonian approach to the two-cavity ZZ system should also accommodate these effects as they would be internal to such a model. This means that **it is sufficient for any error metric to incorporate only bus and drop transmission probabilities.**

For a given system design, a key task is to obtain a general figure of merit. For a particular photon frequency and qubit state in such a system, there are two probabilities to consider: bus and drop transmission. These can be compared to the desired probabilities through distance measures for discrete probability distributions. Concretely, for two distributions, p_x and q_x (x indexes the outcomes), which would represent the expected and actual distributions, respectively, a variety of well-known measures can be computed.

Fidelity

$$F = \sum_x \sqrt{p_x q_x}$$

Trace Distance

$$TD = \frac{1}{2} \sum_x |p_x - q_x|$$

Inner Product

$$IP = \sum_x p_x q_x$$

Relative Entropy

$$RE = \sum_x p_x \log(p_x/q_x)$$

Jensen-Shannon Divergence

$$JSD = \frac{1}{2} \sum_x [p_x \log(p_x/m_x) + m_x \log(m_x/q_x)], \quad m_x = \frac{p_x + q_x}{2}$$

A large fidelity and inner product are desirable, while the same holds for a small trace distance. Furthermore, the fidelity and inner product are closely related, with the difference being only in how the probabilities are exponentiated. **The relative entropy and Jensen-Shannon divergence are ill-suited for our systems** because they require $p_x = 0$ whenever $q_x = 0$, which is almost never the case for any real-world quantum system. We therefore recommend ignoring these latter two metrics.

These metrics all hold for a particular quantum state. S matrix elements for an arbitrary quantum state $\alpha|\uparrow\rangle + \beta|\downarrow\rangle$ can be computed as:

$$S_{ij} = (\alpha^* \langle \uparrow | + \beta^* \langle \downarrow |) a_j U(t_0, t) a_i^\dagger (\alpha |\uparrow\rangle + \beta |\downarrow\rangle) = |\alpha|^2 S_{ij}^\uparrow + |\beta|^2 S_{ij}^\downarrow$$

So S matrix elements for an arbitrary qubit state is a superposition of the basis S matrix elements. This means that the transmission probabilities are also a combination of the basis probabilities. **An overall metric for all quantum states can therefore reasonably consider only the extremal basis probabilities.**

Note that this discussion assumes that the Hamiltonian, and therefore $U(t_0, t)$, is diagonal in the qubit basis (this also means that the z-basis is special and that this analysis is invalid for e.g. the x-basis). This assumption is warranted based on the scope of this project.

To combine metrics for all states, the worse metric over all the basis states is generally taken. This minimization is justified because the figure of merits being developed in this project are general i.e. application-agnostic; application-specific metrics are beyond the scope of this project. Should a particular algorithm utilise a specific qubit state to a heavier extent, different combination schemes could be considered.

One exception to this minimization is for the so-called Cascaded Inner Product. Here the inner product metric is multiplied across all basis states. This is a generalisation of the p_{max} metric from previous work (Gitt 2021), which applies to only the Z system:

$$p_{max} \sim T_{bus}^{\uparrow} T_{drop}^{\downarrow}$$

This renaming of p_{max} is descriptive as the inner products of basis states can be thought of as representing aggregate probabilities; these probabilities are then cascaded in the all-state metric.

With the metrics combined for all qubit states, they need to finally be agglomerated for all photon frequencies. One simple scheme is to take the maximum (for e.g. fidelity and inner product metrics) or minimum (for e.g. trace distance) metric over all frequencies. In particular, applying maximisation to the cascaded inner product for the Z system is equivalent to the p_{max} metric.

Maximisation and minimisation only account for performance at the ideal frequency. Therefore, to account for performance away from ideal frequency as well, integration of the metric over a specified frequency range can be performed. A final proposed method of combining metrics over frequency is to measure the bandwidth over which the metric is above/below a certain threshold. This could be particularly useful when looking for a range of allowable photon frequencies for successful operation, as many error-correcting schemes fail when the systems are inaccurate beyond a critical limit (Xiruo 2020). Particular connection to specific error-correcting methods is a very complex problem and has consequently been considered as outside the scope of this work. Rather, this project has produced general figures of merit for error from S matrix analysis.

References

Combes, Joshua, Joseph Kerckhoff, and Mohan Sarovar. "The SLH framework for modeling quantum input-output networks." *Advances in Physics: X* 2.3 (2017): 784-888.

Fan, Shanhui, et al. "Channel drop filters in photonic crystals." *Optics express* 3.1 (1998): 4-11.

Fan, Shanhui, et al. "Channel drop tunneling through localized states." *Physical Review Letters* 80.5 (1998): 960.

Gitt, Sebastian. *Modelling photon statistics of cavity QED systems for integrated photonic quantum computing*. Diss. University of British Columbia, 2021.

Trivedi, Rahul, et al. "Few-photon scattering and emission from low-dimensional quantum systems." *Physical Review B* 98.14 (2018): 144112.

Yan, Xiruo, et al. "A quantum computer architecture based on silicon donor qubits coupled by photons." *Advanced Quantum Technologies* 3.11 (2020): 2000011.